ผลของการเติมไนโตรเจนต่อสมบัติการสั่นของฟิล์มบาง GaPN ที่มีปริมาณไนโตรเจนสูง

นายนภดล ตุงใย

วิทยานิพนธ์นี้เป็นส่วนหนึ่งของการศึกษาตามหลักสูตรปริญญาวิทยาศาสตรมหาบัณฑิต
สาขาวิชาฟิสิกส์ ภาควิชาฟิสิกส์
คณะวิทยาศาสตร์ จุฬาลงกรณ์มหาวิทยาลัย
ปีการศึกษา 2558
ลิขสิทธิ์ของจุฬาลงกรณ์มหาวิทยาลัย

EFFECTS OF NITROGEN ADDITION ON VIBRATIONAL PROPERTY
OF HIGH NITROGEN-CONTENT GaPN THIN FILMS

Mr. Noppadon Toongyai

จุฬาลงกรณ์มหาวิทยาลัย
CHULALONGKORN UNIVERSITY
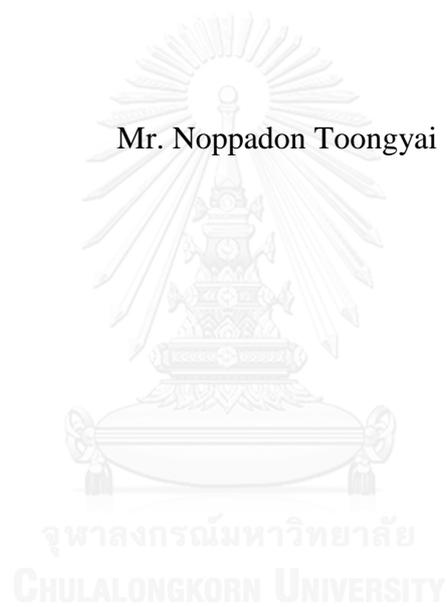
A Thesis Submitted in Partial Fulfillment of the Requirements
for the Degree of Master of Science Program in Physics
Department of Physics
Faculty of Science
Chulalongkorn University
Academic Year 2015
Copyright of Chulalongkorn University

Thesis Title	EFFECTS OF NITROGEN ADDITION ON VIBRATIONAL PROPERTY OF HIGH NITROGEN-CONTENT GaPN THIN FILMS
By	Mr. Noppadon Toongyai
Field of Study	Physics
Thesis Advisor	Assistant Professor Sakuntam Sanorpim, Ph.D.
Thesis Co-Advisor	Associate Professor Songphol Kanjanachuchai, Ph.D.

Accepted by the Faculty of Science, Chulalongkorn University in Partial Fulfillment of the Requirements for the Master's Degree

                    Dean of the Faculty of Science
(Associate Professor Polkit Sangvanich, Ph.D.)

THESIS COMMITTEE

                    Chairman
(Assistant Professor Rattachat Mongkolnavin, Ph.D.)
                    Thesis Advisor
(Assistant Professor Sakuntam Sanorpim, Ph.D.)
                    Thesis Co-Advisor
(Associate Professor Songphol Kanjanachuchai, Ph.D.)
                    Examiner
(Assistant Professor Sojiphong Chatraphorn, Ph.D.)
                    External Examiner
(Somyod Denchitcharoen, Ph.D.)

นภดล ตุงใย : ผลของการเติมไนโตรเจนต่อสมบัติการสั่นของฟิล์มบาง GaPN ที่มี
ปริมาณไนโตรเจนสูง (EFFECTS OF NITROGEN ADDITION ON
VIBRATIONAL PROPERTY OF HIGH NITROGEN-CONTENT GaPN
THIN FILMS) อ.ที่ปรึกษาวิทยานิพนธ์หลัก: สกุลธรรม เสนาะพิมพ์, อ.ที่ปรึกษา
วิทยานิพนธ์ร่วม: ทรงพล กาญจนชูชัย, 55 หน้า.

สมบัติเชิงโครงสร้าง สมบัติการสั่นและสมบัติเชิงแสงของฟิล์ม $GaP_{1-x}N_x$ ที่มีปริมาณ N
(x) จนถึง 5.4 at% และถูกปลูกบนวัสดุฐานรอง GaP ระนาบ (001) ด้วย MOVPE ได้ถูก
ตรวจสอบด้วยการเลี้ยวเบนรังสีเอกซ์กำลังแยกสูง (High Resolution X-Rays Diffraction,
HRXRD), ไมโครรามาน สเปกโทรสโกปี (micro-Raman spectroscopy) และไมโครโฟโตลู
มิเนสเซนต์ (micro-Photoluminescence, micro-PL) ปริมาณ N เฉลี่ยถูกตรวจวัดด้วย
HRXRD มีค่าอยู่ในช่วง 0 ถึง 5.4 at% ชั้นฟิล์มของทุกชิ้นงานอยู่ภายใต้ภาวะความเครียดดึง ผล
การตรวจสอบด้วยกล้องจุลทรรศน์แรงอะตอม (Atomic Force Microscopy, AFM) และกล้อง
จุลทรรศน์อิเล็กตรอนแบบส่องกราด (Scanning Electron Microscopy, SEM) พบผิวหน้าฟิล์ม
และแนวรอยต่อระหว่างชั้นฟิล์มบางและชั้นวัสดุฐานรองมีความเรียบ แม้ชิ้นงานจะมีประมาณ N
มากถึง 5.4 at% ก็ตาม รามานสเปกตรัมได้แสดงโหมดการสั่นที่เกี่ยวกับการเติม N ในโครงผลึก
หรือ N-VMs ในช่วง 440 – 520 cm^{-1} โดยเป็นครั้งแรกที่สามารถยืนยันถึงการมีอยู่ของโหมดการ
สั่นนี้ใน GaPN ที่อุณหภูมิห้อง จากการตรวจสอบ พบว่าความเข้มของ N-VMs จะเพิ่มขึ้นเมื่อเพิ่ม
ปริมาณ N ในฟิล์ม และมีความสัมพันธ์กับปริมาณ N ที่วิเคราะห์ด้วย HRXRD (x_{XRD}) เป็นแบบ
เส้นตรง จากผลดังกล่าวจึงมีความเป็นไปได้ที่จะคำนวณหาปริมาณ N ด้วยวิธีการกระเจิงแบบรา
มาน (x_{Raman}) และดำเนินการเปรียบเทียบค่ากับ x_{XRD} นอกจากนี้ พบว่าค่าช่องว่างแถบพลังงาน
ของ GaPN ที่วิเคราะห์ด้วย micro-PL ที่อุณหภูมิห้อง จะมีค่าลดลงอย่างเห็นได้ชัดเมื่อปริมาณ N
เพิ่มขึ้น โดยมีตัวแปรโบววิง (bowing parameter) สูงถึง 10 eV

ภาควิชา	ฟิสิกส์	ลายมือชื่อนิสิต ....
สาขาวิชา	ฟิสิกส์	ลายมือชื่อ อ.ที่ปรึกษาหลัก ....
ปีการศึกษา	2558	ลายมือชื่อ อ.ที่ปรึกษาร่วม ....

5572009423 : MAJOR PHYSICS

KEYWORDS: GALLIUM PHOSPHIDE NITRIDE / MOVPE / HRXRD / RAMAN SCATTERING / BANDGAP / BOWING PARAMETER

NOPPADON TOONGYAI: EFFECTS OF NITROGEN ADDITION ON VIBRATIONAL PROPERTY OF HIGH NITROGEN-CONTENT GaPN THIN FILMS. ADVISOR: ASST. PROF. SAKUNTAM SANORPIM, Ph.D., CO-ADVISOR: ASSOC. PROF. SONGPHOL KANJANACHUCHAI, Ph.D., 55 pp.

Structural, vibrational and optical properties of $GaP_{1-x}N_x$ films with N contents (x) up to 5.4 at% grown on GaP (001) substrates by MOVPE have been investigated by high resolution X-ray diffraction (HRXRD), micro-Raman spectroscopy and micro-photoluminescence (micro-PL). An average N content was verified by HRXRD to be in a range of 0 to 5.4 at%. All the films are under tensile strain. Smooth surface and fairly flat interface were confirmed by atomic force microscopy (AFM) and scanning electron microscopy (SEM), even though the N atoms were incorporated as high as 5.4 at%. Raman spectra showed the N-related vibrational modes (N-VMs) in range of $440 - 520$ cm^{-1}, which is the first validation for GaPN at room temperature. We have investigated the N-VMs Raman intensity (I_{N-VMs}) as a function of N content determined by HRXRD (x_{XRD}). The I_{N-VMs} was found to rise for the GaPN films with higher N incorporation. It is also evident that the N content in the GaPN films determined by Raman spectroscopy technique (x_{Raman}) exhibits a linear dependence on the x_{XRD}. Our results demonstrate that the linear dependence of x_{Raman} on the x_{XRD} provides a useful calibration method to determine the N content in dilute GaPN films with the N content up to 5.4 at%. Room temperature bandgap determined by micro-PL is dramatically reduced, when the N content is increased. A huge band gap bowing parameter of GaPN is calculated to be 10 eV.

Department:	Physics	Student's Signature	....
Field of Study:	Physics	Advisor's Signature	....
Academic Year:	2015	Co-Advisor's Signature	....

ACKNOWLEDGEMENTS

CONTENTS

LIST OF FIGURES

LIST OF TABLES

CHAPTER I

INTRODUCTION

1.1 Motivations and Purpose

Recently, the group III-V-N semiconductors, such as gallium phosphide nitride (GaPN) and Indium Gallium phosphide nitride (InGaPN) have been greatly attracted attention due to their unique physical properties. Particularly, these are the large bandgap bowing parameter, resulting from an incorporation of a small amount of N [1-4], and the tunable bandgap and lattice constant, which are controlled by adjusting the In and N contents [5, 6]. In practical, GaPN can be grown lattice-matched to a silicon (Si) substrate [7, 8] by adjusting the N content to be 2.0 at%. On the other hand, GaPN also can be coherently grown on a gallium phosphide (GaP) substrate with a few at% of the N incorporation [4, 9]. It is known that GaPN with a small amount of the N content (<1 at%) is a promising material to invent optoelectronics devices operated in the wavelength range of red to green emission. Since, an incorporation of the N plays an important role to enhance a light-operating efficiency, which is due to a formation of momentum-independent energy states located slightly below the conduction band minimum [9-11]. Figure 1-1 shows a schematic diagram of an energy-momentum dispersion relation for the N-contained GaP, demonstrating the momentum-independent energy states established below the X-minima. These energy states are verified to correspond to the N localized states, associated with the N isolated atoms and the NN_i pairs [10-12]. This allows a modification of a type of
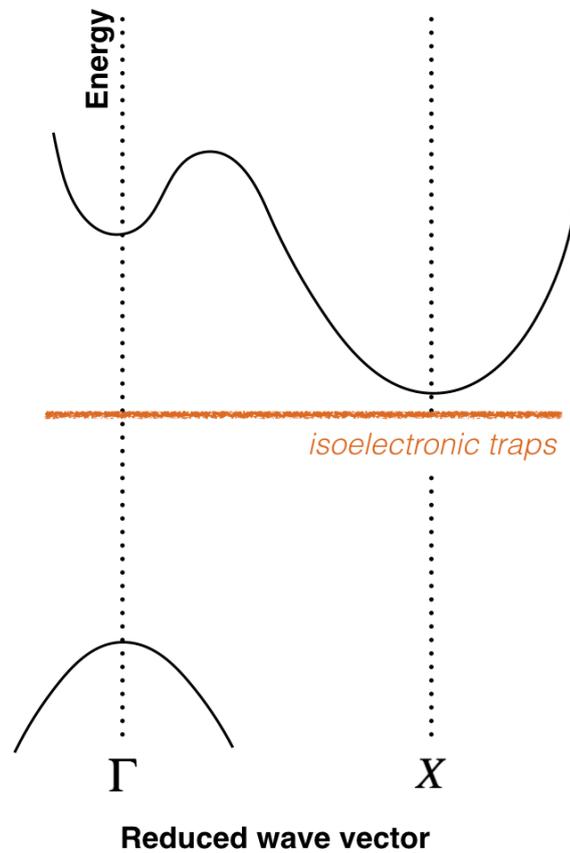
Fig. 1-**1** A schematic diagram of an energy-momentum dispersion relation for the N incorporated GaP with a small amount of N, showing a momentum-independence energy states, namely the isoelectronic traps, which are approximately located at about 10 meV below the X-minima [11].

transition from indirect to direct transition, which creates a direct transition that is an important characteristic of a direct bandgap semiconductor. As a result, GaPN is particularly used as an active layer in light-emitting diodes (LEDs) [13-18] and laser diodes (LDs) [19-21].

Currently, structural and optical properties of high quality GaPN films with the N content up to 3.0 at% have been intensively studied [1, 2, 4, 9-11]. On the other hand, there is only a little reports on optical properties of GaPN with larger N contents (>3.0 at%), because of a limited crystal quality with a high level of the N incorporation. This is probable due to a large miscibility gap between GaP and c-GaN [9, 22]. With addition of N, it is known that the N atoms are almost certainly located in the crystals as point defects, such as the N isoelectronic trap, the NN_i pairs and interstitials, which probably degrade the luminescence efficiency of GaPN films [4, 6, 9]. As a result, in the thesis, we have focused on effects of N addition into high N content GaPN films ($0 \leq N \leq 5.4$ at%), especially GaPN with the N contents higher than 3.0 at%, grown on GaP (001) substrates by metalorganic vapor phase epitaxy (MOVPE).

In order to gain further insight into the nature of point defects emerged from an incorporation of N, we have purposed to investigate crystal vibrational modes which relates to the Ga-N bond by micro-Raman scattering technique. Vibrational modes of the Ga-N bond are an evident that the N atoms are substituted into the P lattice sites to form $GaP_{1-x}N_x$, where x represents a concentration of N in term of at%. Furthermore, the Ga-N bond is also attributed to the N isoelectronic traps in GaPN. Also, we have purposed to use high resolution X-ray diffraction (HRXRD) to determine the N content and strain in the GaPN films with N contents in the range of 0 to 5.4 at%. Finally, micro-Photoluminescence (micro-PL) has been purposed to use for verifying the bandgap of GaPN films at room temperature. The results obtained by micro-Raman spectroscopy, HRXRD and micro-PL measurements will provide further information to accurately predict the bandgap of high N-content GaPN with N contents up to 5.4 at%.

1.2 Objectives

The objectives of the thesis are:

1. To investigate the effects of N incorporation on structural, vibrational and optical properties of high N-content GaPN films grown on GaP (001) substrate by MOVPE.

2. To observe micro-Raman spectra due to the N-related vibrational modes of the GaPN films with different N contents.

3. To verify a relationship between the bandgap of GaPN and N content.

1.3 Organization of the Thesis

The thesis is describing of the investigational results of structural, vibrational and optical properties of high N-content GaPN films with N content in the range of 0 to 5.4 at% grown by MOVPE. The thesis is organized as follows:

Firstly, in **Chapter II**, the basic knowledge and properties of GaPN are described, including basic understanding of the main characterization techniques such as micro-Raman spectroscopy, HRXRD and micro-PL measurements.

In **Chapter III**, the details of GaPN sample's structure, experiments and analyzations are described.

Chapter IV illustrates the investigational results of structural, vibrational and optical properties of high N content GaPN films with the N content up to 5.4 at% using various techniques, which are scanning electron microscopy (SEM), atomic force microscopy (AFM), micro-Raman spectroscopy, HRXRD and micro-PL. Effects of

N addition is analyzed to verify the structural property, N-related vibrational modes and a relationship between the bandgap of GaPN versus the N content.

Finally, **Chapter V** presents the conclusions of the thesis.

CHAPTER II

BASIC KNOWLEDGES OF GaPN

2.1 General properties of GaPN

GaPN, which is a member of a group III-V-Nitrides semiconductors, generally crystalize in zincblend structure. It is produced by a substitution of N atoms in the P lattice sites of the GaP crystal. Figure 2-1 displays crystal structure of GaPN, showing that the N atom substitutes in the (1/4, 1/4, 1/4) P lattice site.
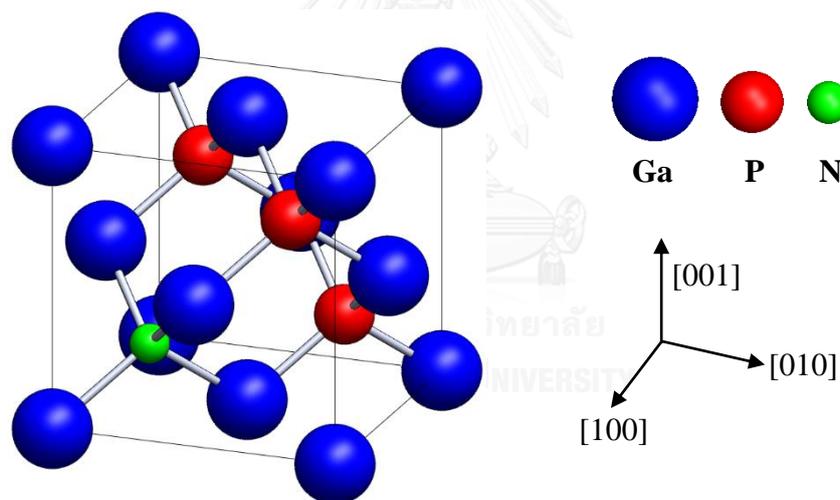
Fig. 2-1 Crystal structure of GaPN. Blue (biggest), red (middle) and green (smallest) balls represent the Ga, P and N atoms, respectively.

GaPN is known as a ternary alloy, which is produced from two binary compounds, GaP and c-GaN. Based on Vegard's law, physical parameters of the ternary alloy is a linear dependent on N content (x). Therefore, the material parameters (P),

such as lattice parameter and elastic properties, of the GaP$_{1-x}$N$_x$ alloy can be calculated using interpolation method [22] as follows:

$$P_{GaPN} = (1-x) \cdot P_{GaP} + x \cdot P_{c-GaN},$$ (2-1)

which is known as Vegard's law. Noted that this formula is suitable for calculate structural parameters, such as lattice parameters and stiffness constants of crystal, because these parameters exhibit linear relationship to material composition (x). However, bandgap of III-V-N ternary alloy, such as GaAsN and GaPN, is dramatically decreasing with N content (x). This behavior shows quadratic relationship between bandgap and the N content, as follows:

$$E_g^{GaPN} = (1-x) \cdot E_g^{GaP} + x \cdot E_g^{c-GaN} - b \cdot x \cdot (1-x),$$ (2-2)

where b is bowing parameter. This parameter is very large for the group III-V-Nitrides semiconductors with respect to the conventional III-V semiconductors, such as InGaAs and GaPAs ternary alloys. This unique behavior is useful to adjust the suitable bandgap of the ternary alloy with a small amount of N. Some structural and optical parameters of GaP and c-GaN are represented in table 2-1 [23]. Previously, Bi, *et.al.,* have studied optical properties of GaPN with N content as high as 16% using absorption measurement [3] and reported that despite a large bandgap bowing existed in GaPN, the alloy still exhibits semiconductor character.

Table 2-**1** Some structural and optical parameters of GaP and c-GaN alloy determined at room temperature.

Parameters	GaP	c-GaN
a_0 (Å)	5.451	4.503
E_g (eV)	2.35 (indirect)	3.30 (direct)
C_{11} (10^{11} dyn/cm^2)	14.1	29.3
C_{12} (10^{11} dyn/cm^2)	6.20	15.9

2.2 The N Isoelectronic Traps

Thomas et.al. discovered the luminescence behavior of isoelectronic electron traps due to pairs of N atoms (NN$_i$ pairs). The NN$_i$ pairs are defined as pairs of N atoms with several separations at P lattice sites [12]. For instance, the pair of N atoms that are located at the nearest neighbor is called NN$_1$ pair. NN$_2$, NN$_3$, NN$_4$ and so on are defined for pairs of N atoms that located at the next and next nearest neighbors, respectively. Figure 2-2 shows schematic diagram of NN$_1$ and NN$_2$ pairs. When the N atoms in pair is largely separated, this situation will be called NN$_\infty$ pair or the isolated N atom. Yaguchi et.al. demonstrated that the isolated N atoms in the GaP crystal occurs when the separation between N atoms are more than 20 Å or 3-4 conventional unit cells of GaP [24]. Energy states of bound excitons due to the NN$_i$ pairs were also measured at low temperature. Figure 2-3 displays the traps energy levels of bound excitons due to the NN$_i$ pairs [12].
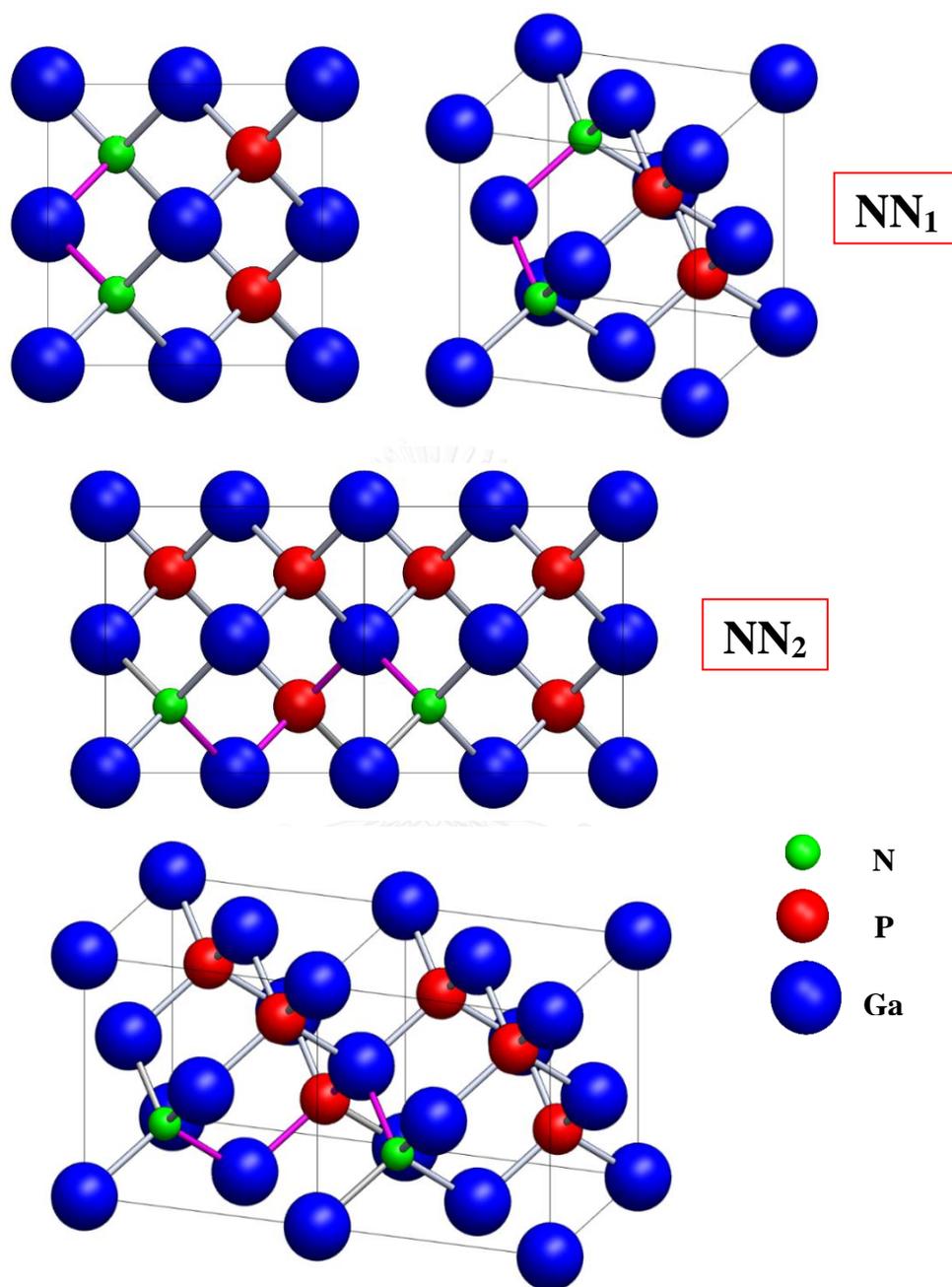
Fig. 2-2 Schematic diagram showing atomic configuration of NN_1 and NN_2 pairs in the GaP crystals.
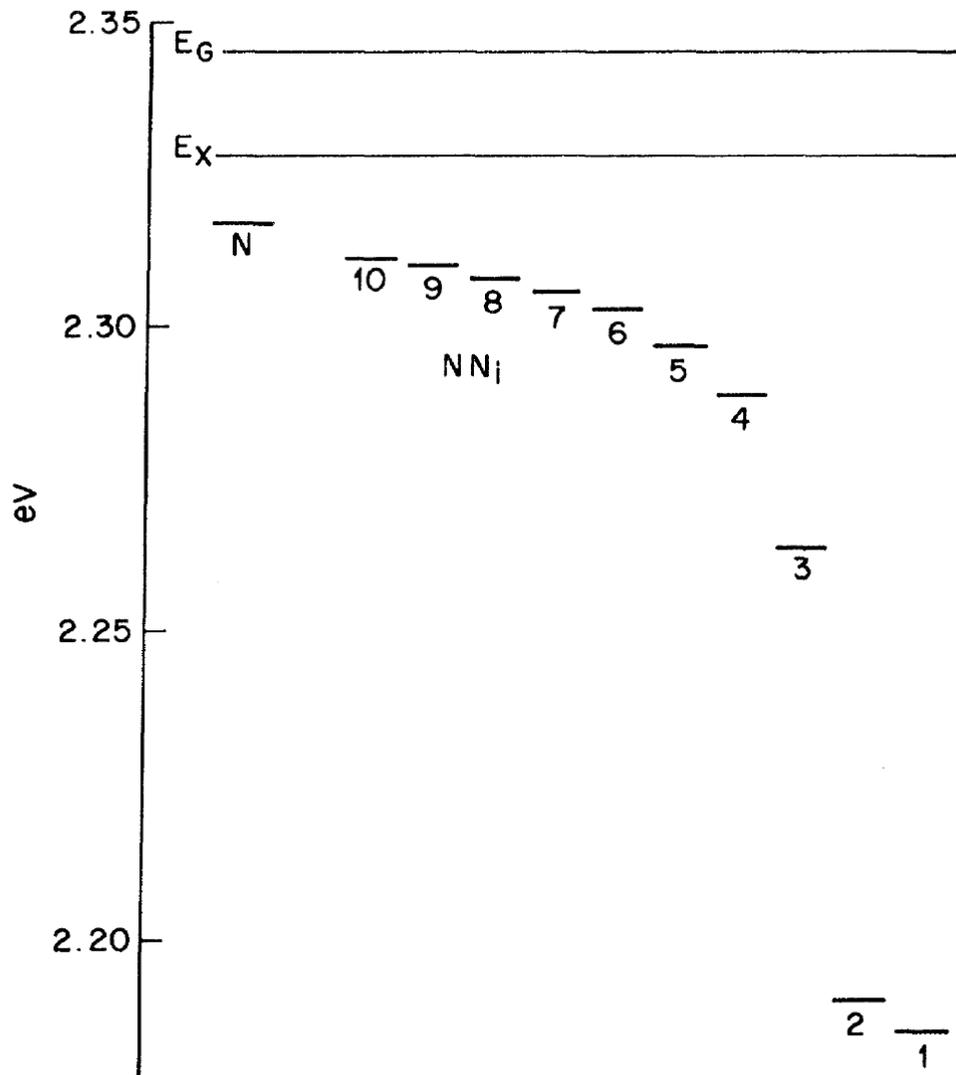
Fig. 2-3 Energy states of bound excitons due to NNi pairs, E_G and E_X represent the minimum energy states of indirect band edge and free exciton. In addition, N is labelled as the energy state of isolated N atom (NN_∞).

2.3 Vibrational modes in GaP

Another characteristic property of solid is the crystals vibration. In quantum representation, the crystals vibrational energy are quantized as phonon and the value of phonon energy is depended on a vibrational frequency of the crystal. Because a primitive unit cell of GaP consists of 2 atoms, Ga and P. Therefore, GaP structure definitely has 6 vibrational branches. These vibrational modes are separated as two transverse acoustic (TA) phonons, two transverse optical (TO) phonons, one longitudinal acoustic (LA) and one longitudinal optical (LO) phonons. The phonon frequencies can be obtained using several techniques, such as infrared absorption and Raman scattering. Figure 2-4 represents our results of TO and LO phonons of the GaP (001) substrate, which is used as a reference in this work, measured by micro-Raman spectroscopy at room temperature in backscattering orientation. GaP-TO and GaP-LO at the zone center (Γ), which are respectively called as GaP-TO (Γ) and GaP-LO (Γ), were clearly observed at 365 and 401 cm^{-1}, respectively. The spectrum with a narrow full width at half maximum (FWHM) indicates that the GaP substrate used in this work exhibits high quality. In additions, five measurements on the substrate display the same magnitude of GaP-TO (Γ). This reveal that the measurements at different locations use the same geometry orientation. The two-phonon modes are also visible in a range of 440 – 540 cm^{-1}, which were emerged by the generation of two phonons.
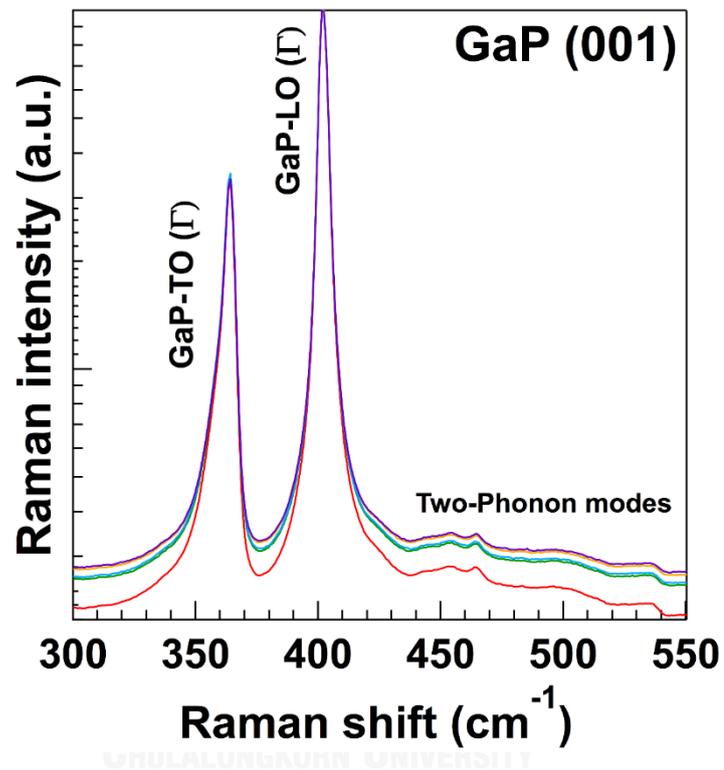
Fig. 2-4 Micro-Raman spectra taken from five positions in the same sample plotted in a logarithmic scale showing transverse and longitudinal optical phonons at the zone center of GaP (001) substrate at room temperature.

2.4 N-Related Vibrational Modes (N-VMs)

Since, a light atom is incorporated in a lattice site and surrounded by larger atoms. A new vibrational mode, which is named as localized vibrational mode (LVM), emerged [25]. For instance, an incorporation of N atoms into the GaAs crystal exhibits a localized N atom surrounded by four Ga atoms, which results in LVM due to a presence of an isolated N atom, as shown in figure 2-5. This vibrational mode is known as N-LVM. Many researchers have studied this N-LVM to confirm the incorporation of N into As lattice sites in the case of GaAsN [26, 27]. Consequently, the finding of the substitutional N atom at group V lattice sites is one of the candidate to be the method for verifying N content. Thus, N content in the ternary III-V-Nitride alloys, such as GaAsN and GaPN, can be verified by an intensity of N-LVM with respect to an inten-
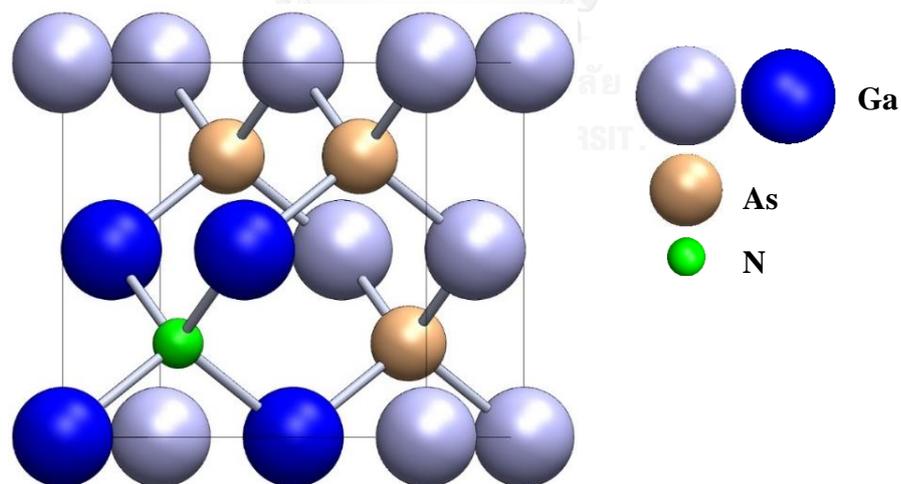
Fig. 2-5 An isolated N atom surrounded by four Ga atoms in the GaAsN alloy.

Table 2-2 The vibrational modes of GaP and the N-related vibrational modes in GaPN.

The vibrational modes	The vibrational frequency (cm^{-1})
GaP-TO (Γ)	365[28]
GaP-LO (Γ)	401[28]
NN_1	491[12]
NN_2	466.5[12]
NN_3	493[12]
NN_4	494[12]
NN_∞	498[12]

-sity of GaP-LO mode. However, an incorporation of N into GaP crystal also induces other N-related vibrational modes (N-VMs), which is due to other NN_i pairs. The vibrational modes of GaP and the N-related vibrational modes in GaPN are listed in table 2-2 as a reference.

CHAPTER III

EXPERIMENTS AND CHARACTERIZATIONS

3.1 Sample Details
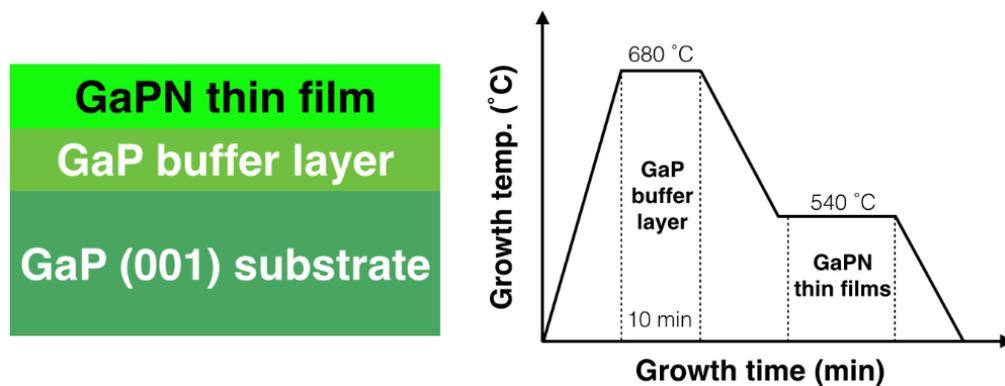
Fig. 3-1 A schematic illustration of sample's structure of GaPN film on GaP (001) substrate and its growth procedures.

GaPN films used in this work were grown on GaP (001) substrate by metalorganic vapor phase epitaxy (MOVPE) at Onabe's laboratory, department of advance materials, University of Tokyo, Japan. Trimethylgallium (TMG), Tertiarybutylphosphine (TBP) and dimethylhydrazine (DMHy) were used as Ga, P and N precursors, respectively. Figure 3-1 represents a schematic illustration of sample's structure of GaPN film grown on GaP (001) substrate and its growth procedures. Firstly, GaP buffer layer was grown for 10 min with the growth temperature of 680 °C. Then GaPN film was grown consecutively with the growth temperature of 540 °C. To vary film thickness, the growth of GaPN film was done at 5 and 10 min. To obtain the GaPN films with different N content. The flow rate of DMHy, [DMHy], was varied in the range of 0 - 300 μmol/min to adjust the N content in the thin films.

3.2 Characterizations

3.2.1. High resolution X-rays diffraction

High resolution X-rays diffraction (HRXRD) is a prevalent method to determine the structural properties of epitaxial films, such as crystals structure, crystals quality, lattice parameters, alloy compositions, lattice mismatch as well as strain properties. HRXRD is also suitable to measure N content in GaPN alloy by obtaining the lattice constants of GaPN films in both directions of perpendicular ($a_\perp$) and parallel ($a_\parallel$) to the GaP (001) substrate surface, using a (004) symmetric and an (115) asymmetric reflections, respectively. HRXRD used in this work was operated using the Bruker-AXS D8 DISCOVER located at the Scientific and technological research equipment center (STREC), Chulalongkorn University. The $K_{\alpha 1}$ characteristic X-rays with wavelength of 1.5406 Å emitted from a copper target was used as the incident X-rays. The (022) channel-cut Ge and the graded mirror were combined in the monochromator to eliminate the $K_{\alpha 2}$ and K_β radiations, respectively. The sample is placed on an Euler cradle, which can adjust the sample alignment to optimize the scattered X-ray beam. In addition, the secondary (022) Ge crystal monochromator is also placed in front of a detector for higher accuracy measurement. The HRXRD set up and instrument have been displays in figure 3-2 and 3-3, respectively.
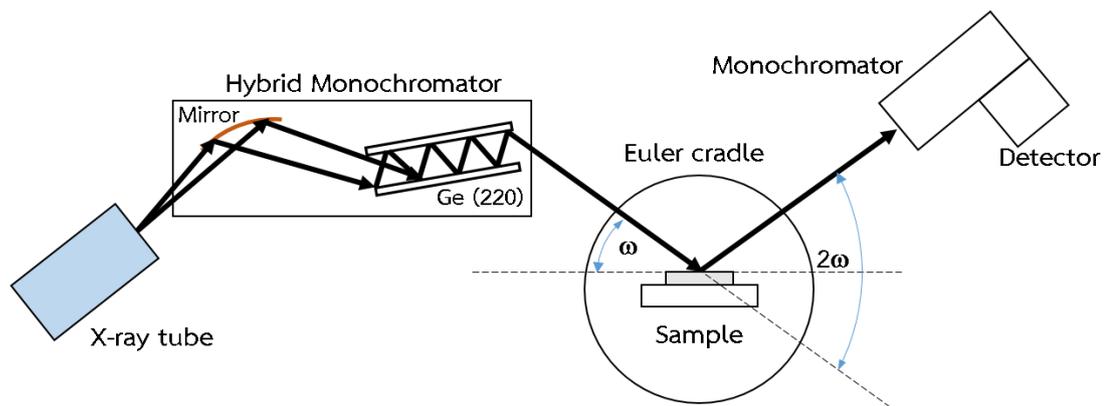
Fig. 3-2 A schematic illustration HRXRD set up.

Fig. 3-3 HRXRD measurement installed at the Scientific and technological research equipment center, Chulalongkorn University.
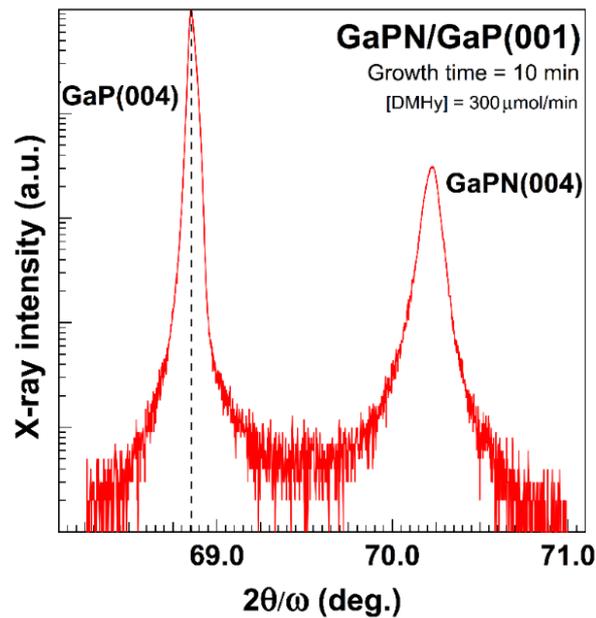
Fig. 3-4 HRXRD pattern of a symmetrical (004) 2θ/ω scan of GaPN film grown on GaP (001) substrate for 10 min with [DMHy] = 300 μmol/min.

For example, figure 3-4 shows HRXRD pattern of a symmetrical (004) reflection of GaPN film grown on GaP (001) substrate for 10 min with [DMHy] = 300 μmol/min. It is clearly seen explicit two diffraction peaks, which are corresponded to the diffraction from substrate and layer indicating as GaP (004) and GaPN (004), respectively. According to Bragg's law, $a_\perp$ can be calculated from Bragg's angle of the films using the angle corresponds to the substrate to be a reference, as follows:

$$2d_{(hkl)}\sin(\theta) = n\lambda \ , \ \ n = 1, 2, 3, \ldots \qquad (3\text{-}1)$$

$$\frac{1}{d_{(hkl)}^2} = \frac{h^2 + k^2}{a_\perp^2} + \frac{l^2}{a_\parallel^2} \ , \qquad (3\text{-}2)$$

It is well known that difference between tile angle of the strain influenced layer and the substrate ($\Delta\omega$) are obviously detected from an asymmetrical (115) reflection using HRXRD via a reciprocal space mapping (RSM) mode. Figure 3-5 shows the (001) and (115) planes of the strain-influenced layer and the substrate. The difference between the tile angles ($\Delta\omega$) between (115) planes of substrate and stain-influenced layer can be calculated as follows:

$$\Delta\omega = \omega_2 - \omega_1 = \tan^{-1}(\frac{\sqrt{2}}{5}) - \tan^{-1}(\frac{\sqrt{2}}{5} \cdot \frac{a_\parallel}{a_\perp}), \qquad (3\text{-}3)$$

where, ω_1 and ω_2 are tile angles of the (115) plane, which is respect to (001) plane, for the substrate and the stain-influenced layer, respectively.
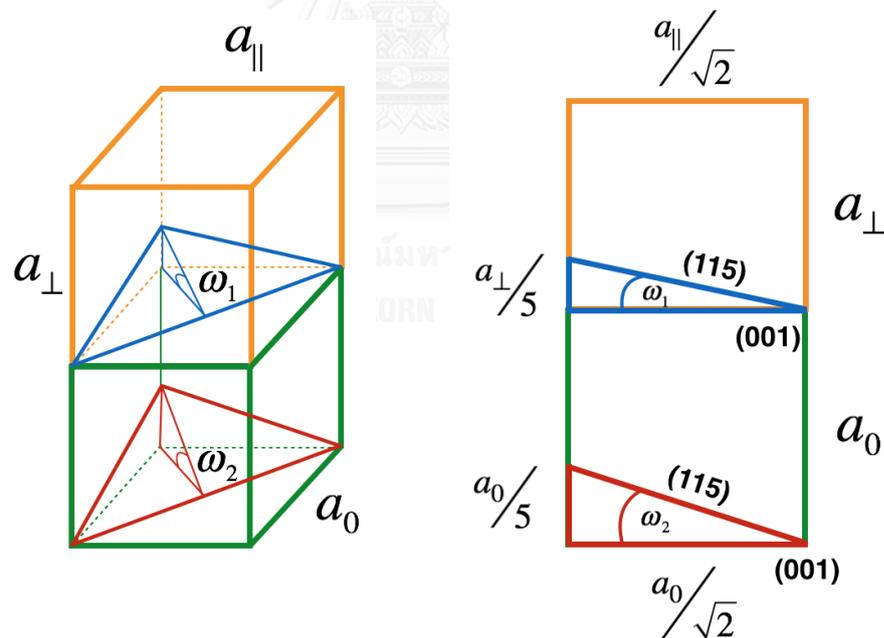
Fig. 3-5 Tile angles of (115) with respect to (001) of the strain-influenced layer and the substrate.
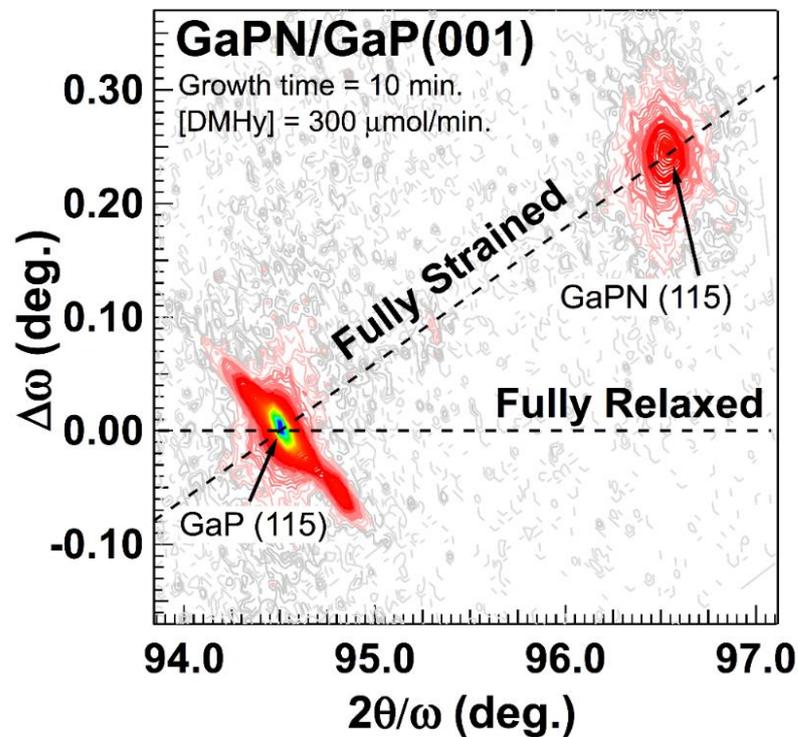
Fig. 3-6 The (115) reciprocal mapping spectrum of GaPN thin film on GaP substrate with [DMHy] = 300 μmol/min and the growth time of 10 min.

Figure 3-6 displays a reciprocal space mapping of an asymmetrical (115) reflection for the corresponding GaPN film grown on GaP (001) substrate for 10 min with [DMHy] = 300 μmol/min. It is clearly to detect the contour mappings of GaPN (115) and GaP (115) reflections with the tile angle $\Delta\omega$ of 0.26°. Based on the values of perpendicular lattice parameter ($a_{\perp}$) and $\Delta\omega$, therefore, parallel lattice parameter ($a_{\parallel}$) is calculated using eq. (3-3).

As a result, the N content (x) of GaP$_{1-x}$N$_x$ can be determined from the average freestanding lattice constant (a_0) as follows:

$$a_0^{GaPN} = \frac{C_{11} \cdot a_\perp + 2C_{12} \cdot a_\parallel}{C_{11} + C_{12}}, \qquad (3\text{-}4)$$

$$a_0^{GaPN} = x \cdot a_0^{c-GaN} + (1-x) \cdot a_0^{GaP}, \qquad (3\text{-}5)$$

$$C_{11} = \frac{x \cdot a_0^{c-GaN} \cdot C_{11}^{c-GaN} + (1-x) \cdot a_0^{GaP} \cdot C_{11}^{GaP}}{a_0^{GaPN}}, \qquad (3\text{-}6)$$

$$C_{12} = \frac{x \cdot a_0^{c-GaN} \cdot C_{12}^{c-GaN} + (1-x) \cdot a_0^{GaP} \cdot C_{12}^{GaP}}{a_0^{GaPN}}, \qquad (3\text{-}7)$$

where a_0^{GaP} and a_0^{c-GaN} are the freestanding lattice constants of GaP and c-GaN, respectively. In additions, C_{11} and C_{12} are stiffness constants of GaPN thin films. Those four equations are necessary to be used to estimate the N content in GaPN thin films via an iteration method. For first loop, the values of C_{11} and C_{12} of GaP were used as input for the calculation.

3.2.2. Raman scattering

When single wavelength photons were applied to the crystal lattices, some photons probably scatter with elastic and inelastic processes. Scattered photons in an inelastic process contain energy which differ from the energy of incident photons. An appearance of energy difference exists due to lattice vibration and this inelastic scattering is called Raman scattering. The angular frequencies (ω) and the wavevectors (k) of the first-order Raman scattering are described as:

$$\omega_i = \omega_s + \omega_{phonon}$$

$$k_i = k_s + k_{phonon}$$

$$\omega_i = \omega_s - \omega_{phonon}$$
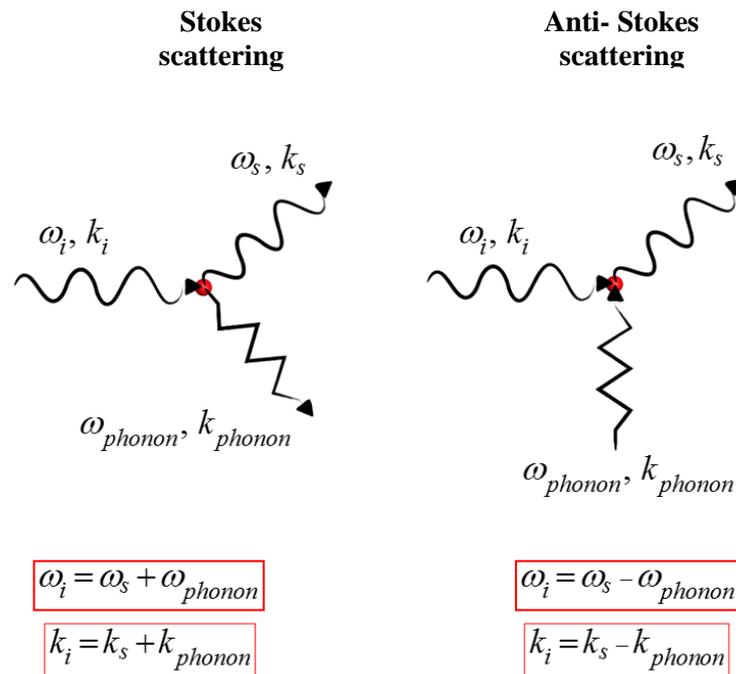
$$k_i = k_s - k_{phonon}$$

Fig. 3-7 Diagrams of Stokes and anti-Stokes scattering processes.

$$\omega_i = \omega_s \pm \omega_{phonon}, \qquad (3\text{-}8)$$

$$k_i = k_s \pm k_{phonon}, \qquad (3\text{-}9)$$

where i and s represent the parameters of incident and scattered photons and ω_{phonon} and k_{phonon} represent the angular frequency and wavevector of phonon gained (-) or lose (+) in the crystals. Figure 3-7 illustrates of Stoke and anti-Stoke processes of the first order Raman scattering. The scattering process with gained or lose phonon in the crystals are named as Stokes and anti-Stokes scattering, respectively. Generally, phonon energy obtained from both processes are presented in the same magnitude but scattered photon intensity from Stokes scattering is much higher than that of anti-Stokes scattering. This makes the spectra observed from anti-Stokes scattering must be measured at high temperature to gain photon energy from phonon energy (lattice vibration) of the system,
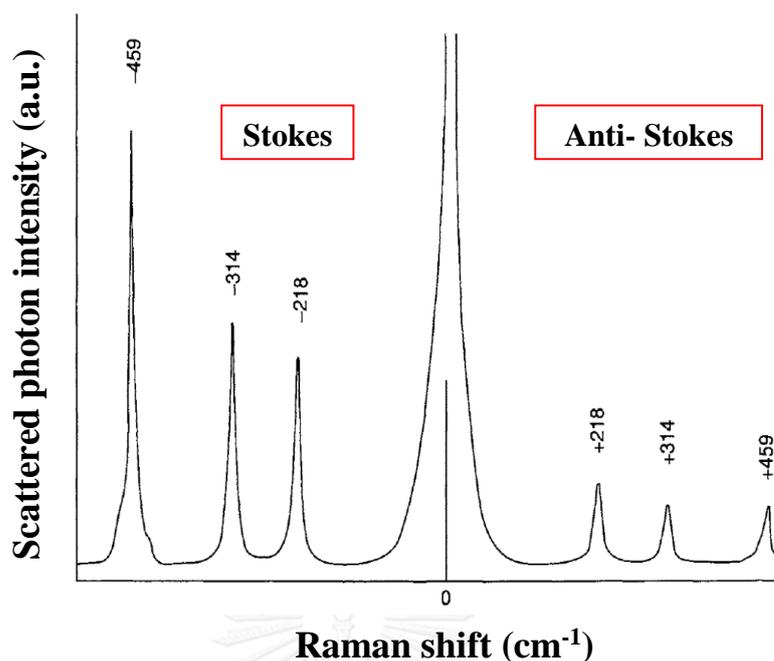
Fig. 3-8 Schematic illustration of Stokes and anti-Stoke scattering of some material, showing as an example, using 488.0 nm-laser as the excitation source.

as shown in figure 3-8. Therefore, Stoke scattering is a suitable process to measure Raman spectra at room temperature. The results obtained from Raman spectroscopy are obviously plot between the scattered photon intensity as a function of the energy difference, between the scattered photon energy and the excitation energy, in the unit of wavenumber (cm^{-1}). Practically, the scattered photon intensity and energy difference are called as Raman intensity and Raman shift, respectively.

Raman spectroscopy used in this work was carried out using NT-MDT NTE Spectra micro-Raman spectroscopy at National Nanotechnology Center (NANOTEC), National Science and Technology Development Agency (NSTDA). The backscattering orientation and the room temperature were selected to probe the scattered photon using the 632.8 nm-laser as the excitation source. The beam diameter of the excitation source

is about 2 µm. The results were recorded for 5 times at difference locations and the measurement range was 150 – 900 cm^{-1} to cover the Raman shift of the second order mode of GaP-LO (Γ). The Raman spectroscopy set up and instrument have been displays in figure 3-9 and 3-10, respectively.
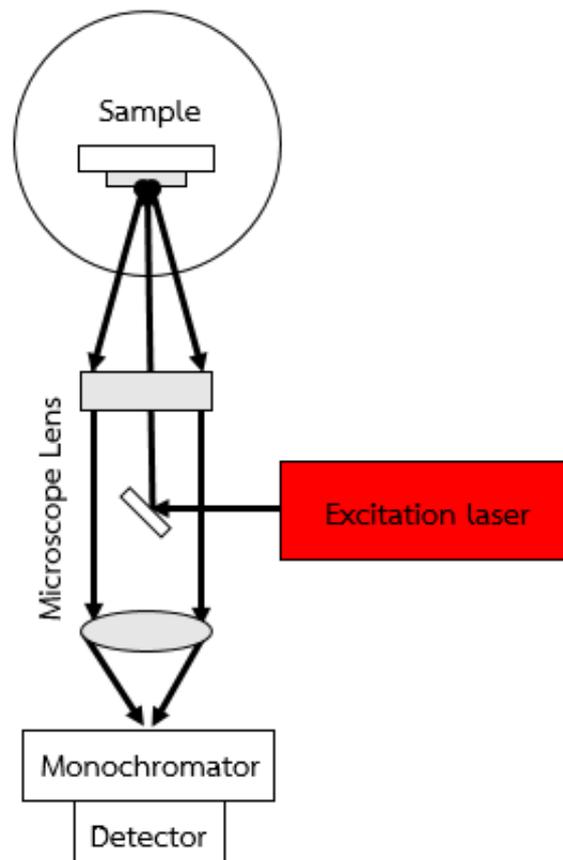
Fig. 3-9 A schematic illustration of Raman spectrometer set up.

Fig. 3-10 Raman spectroscopy installed at National Nanotechnology Center (NANOTEC), National Science and Technology Development Agency (NSTDA).

3.2.3. Photoluminescence

Monochromatic light, which contains energy higher than energy band gap of the sample, is focused onto the sample. The sample will absorb the photon and electron in the sample are excited to the conduction band. When the excited electrons are recombined to valence band, some energy is released through photons with energy equal to the energy difference between the excited energy states and the valence band. The released photons can give useful information as band gap energy, impurity energy levels, recombination mechanism and sample quality. Because the excitation source is photon, therefore this technique is called Photoluminescence. Micro-photoluminescence spectroscopy which was used in the thesis was operated at room temperature by Renishaw RM1000 at the Gem and Jewelry Institute of Thailand (Public organization). The 532-nm monochromatic light was selected as the excitation source.

CHAPTER IV

RESULTS AND DISCUSSION

In this chapter, the GaPN films grown on GaP (001) substrates were characterized using various measurements as mentioned in the previous chapter. Effects of N addition are analyzed to verify the structural properties, N-related vibrational modes and a relationship between the bandgap of GaPN and N content.

4.1 Structural Investigations

4.1.1 Determination of N content

In order to obtain N content in the GaPN films with various flow rates of DMHy, high resolution X-ray diffraction (HRXRD) measurements were performed using $2\theta/\omega$-scan and reciprocal space mapping (RSM) modes. For GaPN on GaP (001), a symmetrical (004) $2\theta/\omega$-scan and an asymmetrical (115) RSM are required to measure the lattice parameters ($a_\perp$ and $a_\parallel$) of the GaPN thin films.

Figure 4-1 shows HRXRD $2\theta/\omega$ profiles of GaPN films grown on GaP (001) substrates for 5 and 10 min with various flow rates of DMHy. The peak that corresponds to the GaP substrate is constrained at 68.874° when assume that the lattice constant of GaP substrate is constant ($a_0 = 5.451$ Å). It is clearly seen that the GaPN peaks in the both figures are located at higher diffraction angles with respect to the GaP peak.
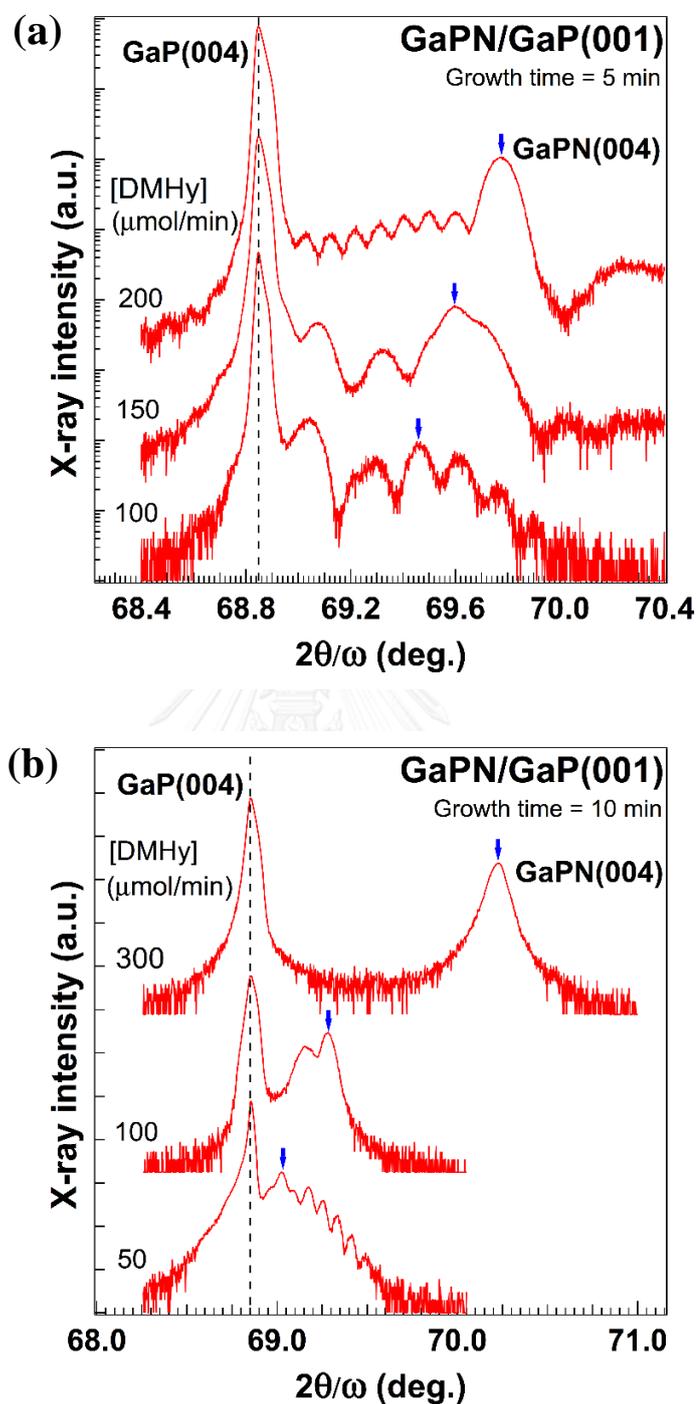
Fig. 4-1 HRXRD (004) 2θ/ω profiles of GaPN films grown on GaP (001) substrates for (a) 5 and (b) 10 min with various DMHy flow rates.

Table 4-1 Perpendicular lattice parameter ($a_\perp$) and its distribution ($\Delta a_\perp$) of GaPN

films grown on GaP substrates for 5 and 10 min with various DMHy flow rates.

Growth time	5 min			10 min		
[DMHy] (μmol/min)	100	150	200	50	100	300
$a_\perp$ (Å)	5.408	5.399	5.387	5.438	5.421	5.357
$\Delta a_\perp$ (Å)	0.04	0.05	0.06	0.01	0.03	0.09
$\Delta a_\perp / a_\perp$ (%)	0.74	0.93	1.10	0.18	0.55	1.70
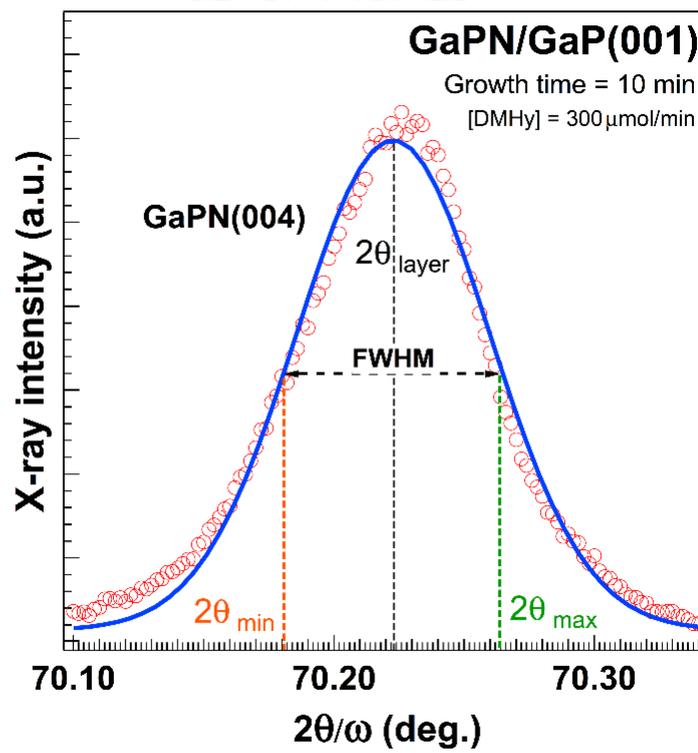
Fig. 4-2 XRD peak of GaPN (004) showing a peak position ($2\theta_{layer}$) and a FWHM

($2\theta_{max} - 2\theta_{min}$) for the film with [DMHy] = 300 μmol/min and growth time of 10 min.
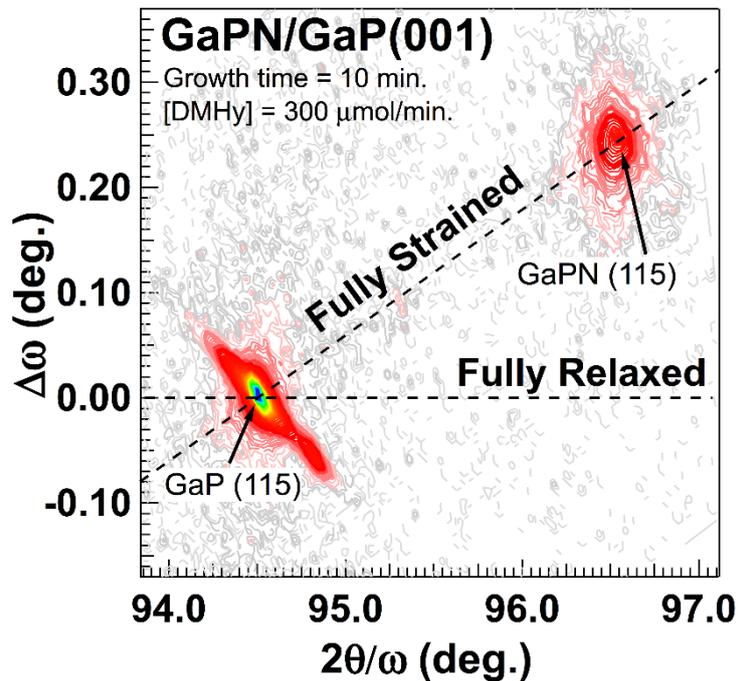
Fig. 4-3 HRXRD reciprocal space mapping of the asymmetrical (115) reflection of GaPN film grown on GaP (001) substrate for 10 min with [DMHy] = 300 μmol/min.

This results indicate that the lattice constant of GaPN thin films is smaller than that of GaP substrate, indicating that all the GaPN thin films are under tensile strain. Perpendicular lattice parameter ($a_\perp$) of GaPN thin films were calculated as illustrated in table 4-1. The values of its distribution ($\Delta a_\perp$), which were calculated from full width at half maximum (FWHM) of the diffraction peak, are also listed in this table 4-1. As an example, as shown in figure. 4-2, XRD peak of GaPN (004) was fitted using Gaussian's distribution, indicating peak position ($2\theta_{layer}$) and FWHM ($2\theta_{max} - 2\theta_{min}$), which were used to calculate the value of $a_\perp$ and its distribution $\Delta a_\perp$, respectively.

As mentioned previously, the parallel lattice parameter ($a_\parallel$) is also necessary for determination of N content in the GaPN thin films. As described in Chapter 3, this lattice parameter can be obtained using reciprocal space mapping (RSM) of the asymmetrical (115) reflection. Figure 4-3 illustrates the HRXRD RSM of (115) reflections of GaPN thin film grown on GaP (001) substrate for 10 min using [DMHy] = 300 µmol/min, which is the highest DMHy flow rate used in this work. Obeying the Bragg's law, diffraction peak located at the left and bottom of the contour plot is corresponded to the GaP (115) reflection. When the thin films were grown epitaxially, it is obviously to observe another dominant diffraction peak indicating the GaPN (115) reflection, which is located at the right and top of the contour plot. As shown in the figure, the diffraction peak of GaPN (115) is located closely the fully strain-line and the tile angle ($\Delta\omega$) between the layer and substrate is measured to be 0.245°. Using the values of $\Delta\omega$ and $a_\perp$, the value of $a_\parallel$ was calculated to be 5.446 Å. It is found that the value of $a_\parallel$ of GaPN film and that of GaP substrate are slightly different (~0.09%). This value is much smaller than the value of lattice distribution ($\Delta a_\parallel / a_\parallel = 0.37\%$). This implies that the GaPN grown films are under the fully tensile strain. In addition, the value of $\Delta a_\parallel$ are also present using the same interpretation as the $\Delta a_\perp$. The values of $a_\parallel$ and $\Delta a_\parallel$ of GaPN films grown on GaP (001) substrates for 5 and 10 min with DMHy flow rates in the range of 100 to 300 µmol/min are listed in the table 4-2.

Table 4-2 Parallel lattice parameter ($a_{\parallel}$) and its distribution ($\Delta a_{\parallel}$) of GaPN films grown on GaP (001) substrates for 5 and 10 min with various DMHy flow rates.

Growth time	5 min			10 min		
[DMHy] (µmol/min)	100	150	200	50	100	300
$a_{\parallel}$ (Å)	5.451	5.451	5.451	5.448	5.449	5.446
$\Delta a_{\parallel}$ (Å)	0	0	0	0.007	0.006	0.02
$\Delta a_{\parallel} / a_{\parallel}$ (%)	0	0	0	0.13	0.12	1.83

The results shown in the table 4-1 and 4-2 were used to further verify the N content in the GaPN thin films. Also, some structural parameters were determined. Table 4-3 summaries the structural parameters, such as lattice parameters, elastic constants and N contents, which were determined by HRXRD. As seen in table 4-3, x_{XRD} and Δx_{XRD} represent the N content and its distribution. The highest N content is 5.4 ± 0.6 at% for the GaPN film with the highest DMHy flow rate of 300 µmol/min.

Table 4-3 Calculated structural parameters of GaPN films grown on GaP (001) substrates for 5 and 10 min with DMHy flow rate in the range of 100 to 300 μmol/min are listed. Noted that x_{XRD} represents the N content, which is determined by HRXRD. The value of Δx_{XRD} indicates a distribution or a fluctuation of N content.

Growth time	5 min			10 min		
[DMHy] (μmol/min)	100	150	200	50	100	300
$a_\perp$ (Å)	5.408	5.399	5.387	5.438	5.421	5.357
$a_\parallel$ (Å)	5.451	5.451	5.451	5.448	5.449	5.446
a_0 (Å)	5.428	5.423	5.417	5.443	5.434	5.399
C_{11} (10^{11} dyn/cm^2)	13.9	13.8	13.7	14.0	13.9	13.6
C_{12} (10^{11} dyn/cm^2)	6.14	6.09	6.07	6.17	6.14	5.99
in-plane mismatch (%)	0	0	0	-0.055	-0.037	-0.092
lattice mismatch (%)	-0.410	-0.514	-0.624	-0.147	-0.312	-0.954
x_{XRD} (at%)	2.4	2.9	3.6	0.8	1.8	5.4
Δx_{XRD} (at%)	0.4	0.4	0.2	0.2	0.2	0.6

4.1.2 Surface and Interface Morphologies

Figure 4-4 shows surface morphologies of GaPN thin films grown on GaP (001) substrates for (a) – (c) 5 min and (d) – (f) 10 min with various DMHy flow rates. It is clearly seen that there are no cracks on the surface for the N contents lower than 3.6 at%. However, a micro crack, which is visible as a line contrast, was observed on GaPN with N containing of about 5.4 at%. This micro crack was generated by

a degradation of the layer interface due to a large lattice mismatch. Figure 4-5 illustrates atomic force microscopy (AFM) images for surface morphologies of the corresponded GaPN thin films. As shown in figures 4-5 (a) – (c), AFM images of GaPN films with the growth time of 5 min exhibited small grain sizes and smoother surfaces with root mean square (RMS) roughness of 0.3 nm for the N contents lower than 2.9 at%. As an expectation, surface roughness was significantly gained to RMS roughness of 1.3 nm when the N content is increased to 3.6 at%. On the other hand AFM images of GaPN thin films grown for 10 min exhibited flat surfaces with RMS roughness of 0.5 nm for the N contents up to 5.4 at%. However, the surface of the film with the N content of 5.4 at% was also occupied by ~ 3.0 nm-pits, which were randomly distributed on the surface.

Figure 4-6 displays the interface of GaPN films and GaP (001) substrates for the corresponding samples shown in figure 4-4 and 4-5 using FE-SEM in backscattering electron mode. Fairly flat interface was clearly observed for all the samples. With higher N incorporation, the film thickness was found to decrease, as summarized in the table 4-4. According to these results, it is confirmed that the film quality is good enough for further analyses that are the vibrational and optical investigations.
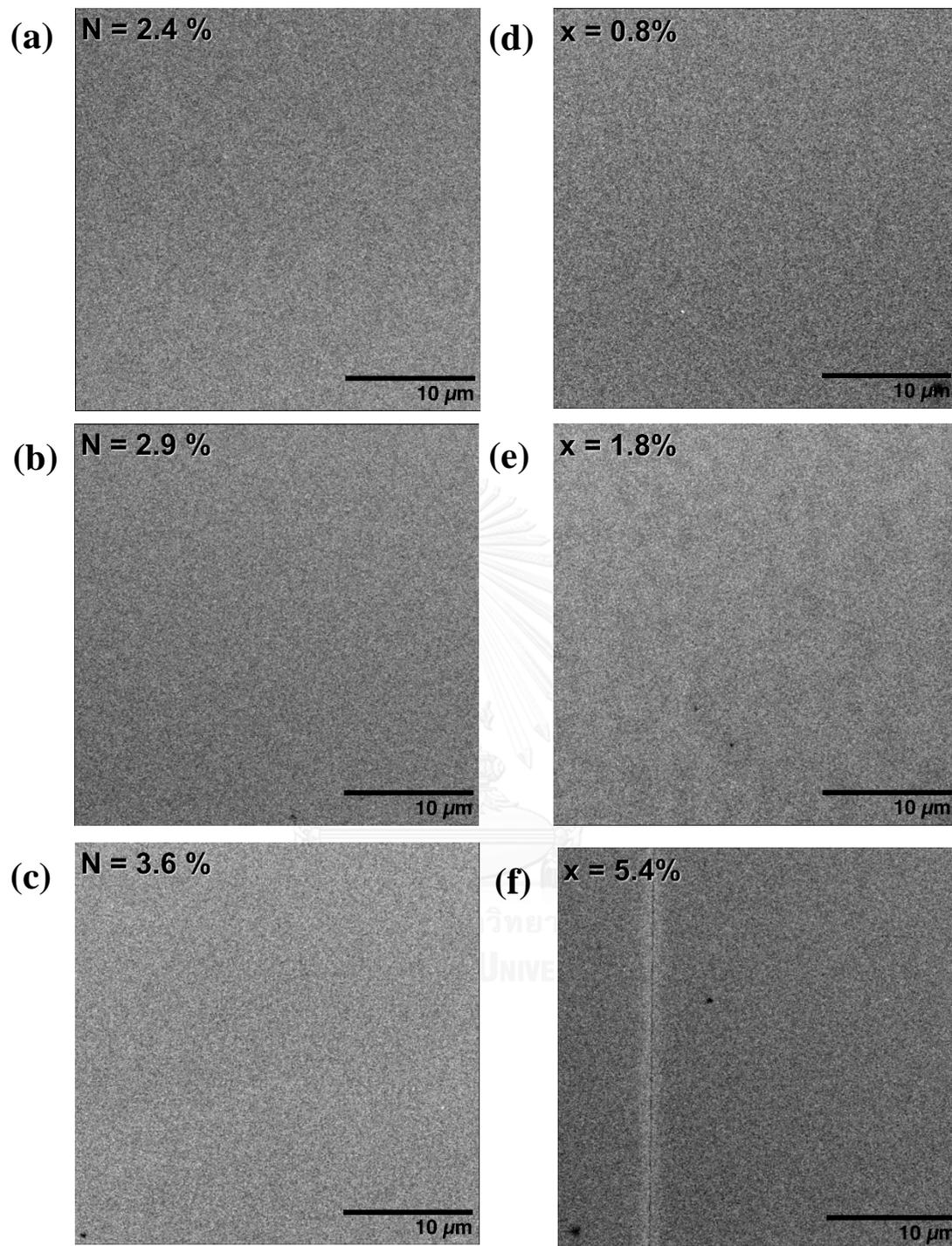
Fig. 4-4 SEM images showing surface morphologies of GaPN films grown on GaP (001) substrates for (a) − (c) 5 and (d) − (f) 10 min with various DMHy flow rates.
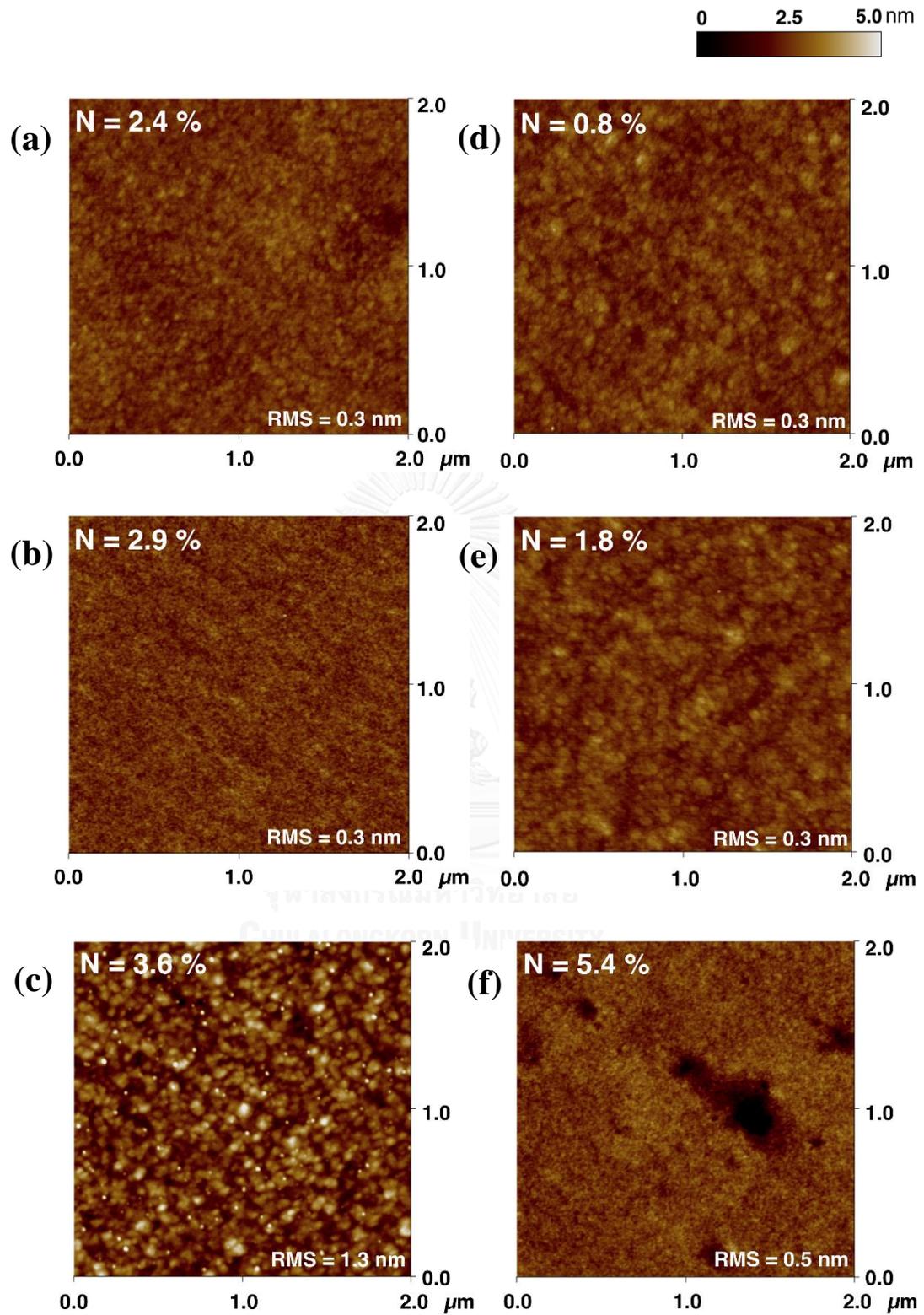
**Fig. 4-5** AFM images showing surface morphologies of GaPN films grown on GaP (001) substrates for (a) – (c) 5 and (d) – (f) 10 min with various DMHy flow rates.
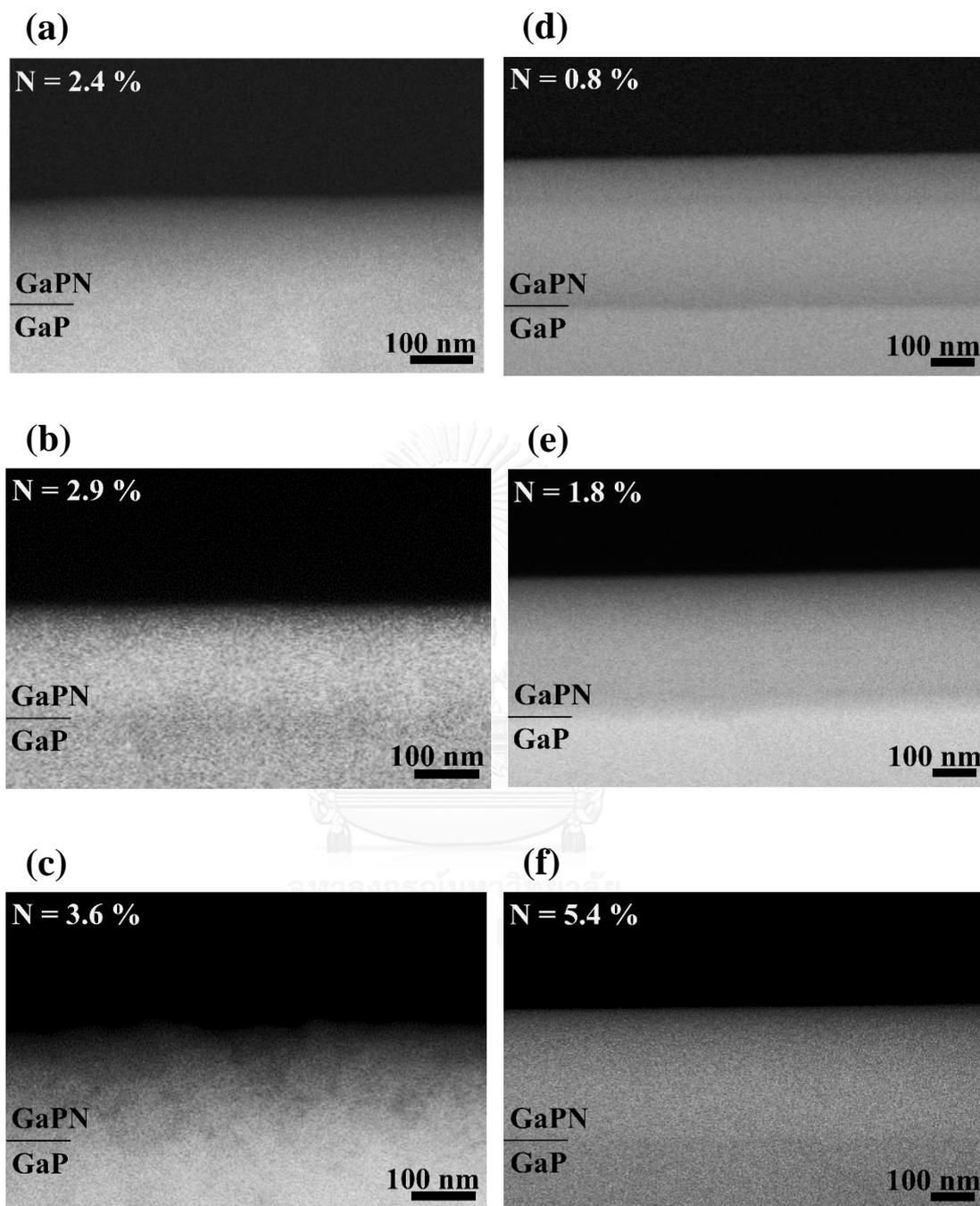
Fig. 4-6 Cross-sectional FE-SEM images showing interface between GaPN and GaP for the films grown for (a) – (c) 5 and (d) – (f) 10 min with various DMHy flow rates.

Table 4-4 Film thickness and RSM roughness were respectively obtained from cross-sectional FE-SEM and AFM images of GaPN thin films on GaP substrates for 5 and 10 min with various DMHy flow rates. S.D. is a standard deviation calculated from 20 times of thickness measuring for different regions of the films.

Growth time	5 min			10 min		
N content (x_{XRD}, at%)	1.8	2.9	3.6	0.8	1.8	5.4
Thickness (nm)	177	172	167	347	327	317
S.D. (nm)	4	2	9	4	10	2
RSM roughness (nm)	0.3	0.3	1.3	0.3	0.3	0.5

4.2 Vibrational Investigations

4.2.1 N-Related Vibrational modes

Figure 4-7 illustrates normalized micro-Raman spectrum of GaPN thin films with the highest N content of 5.4 at% taken in a backscattering configuration at room temperature. Micro-Raman spectrum of GaP substrate was also recorded as a reference for comparison. For the spectrum of GaP, it is clearly observed that GaP-TO (Γ) and GaP-LO (Γ) phonon modes are appeared at 365 and 401 cm^{-1}, respectively. Since, the GaP-TO (Γ) phonon mode is a forbidden mode for the backscattering configuration. Therefore, the GaP-TO (Γ) in GaP might be emerged due to several effects such as misorientation geometry measurement and imperfect crystal alignment. Moreover, the Ga-P bonds related two phonon modes are also observed in a range of 440 to 520 cm^{-1} [29, 30]. For GaPN with N content of 5.4 at%, the GaP-TO (Γ) and GaP-LO (Γ) phonon modes were also detected. With incorporation of N, the intensity

of GaP-TO (Γ) phonon mode of GaPN became larger than that of GaP. Thus, this result suggests that the quality of GaP structure is degraded due to a lattice distortion with an incorporation of N. Furthermore, additional features were observed were detected at 391 cm^{-1} and in a range of 440 – 520 cm^{-1}. These features emerged when the N content is increased.
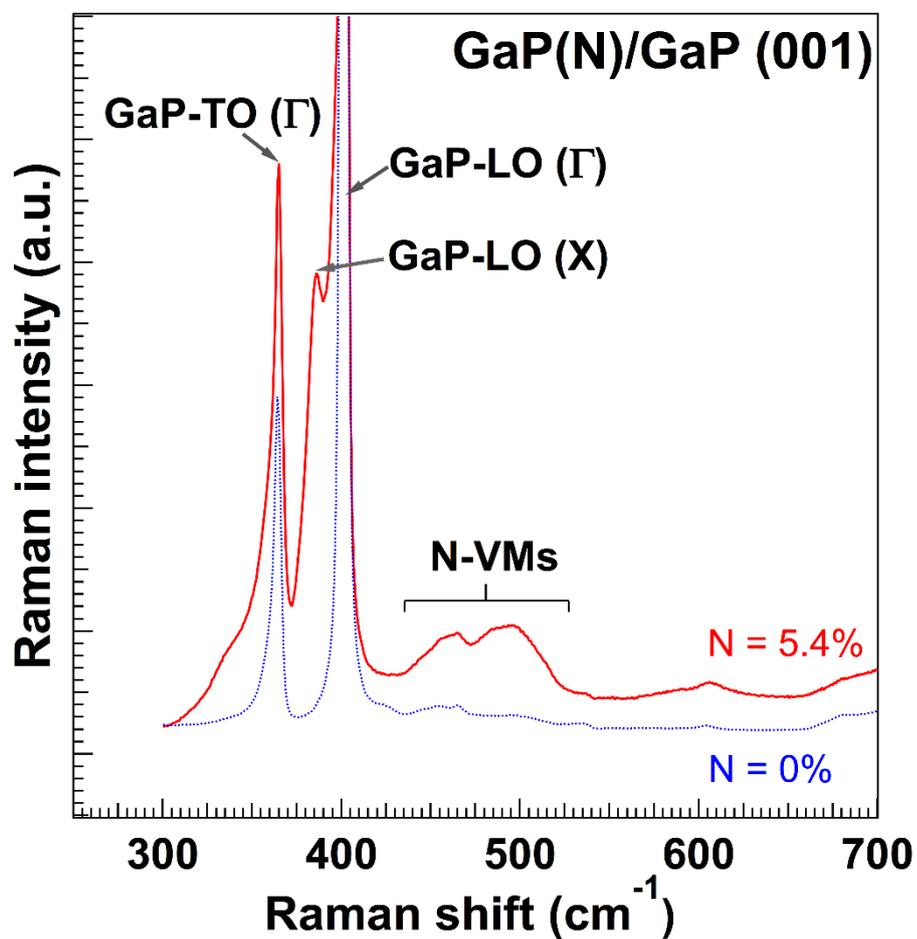
Fig. 4-7 Micro-Raman spectra of GaP buffer layer (blue dotted line) and GaPN film with the highest N content of 5.4 at% (red solid line).
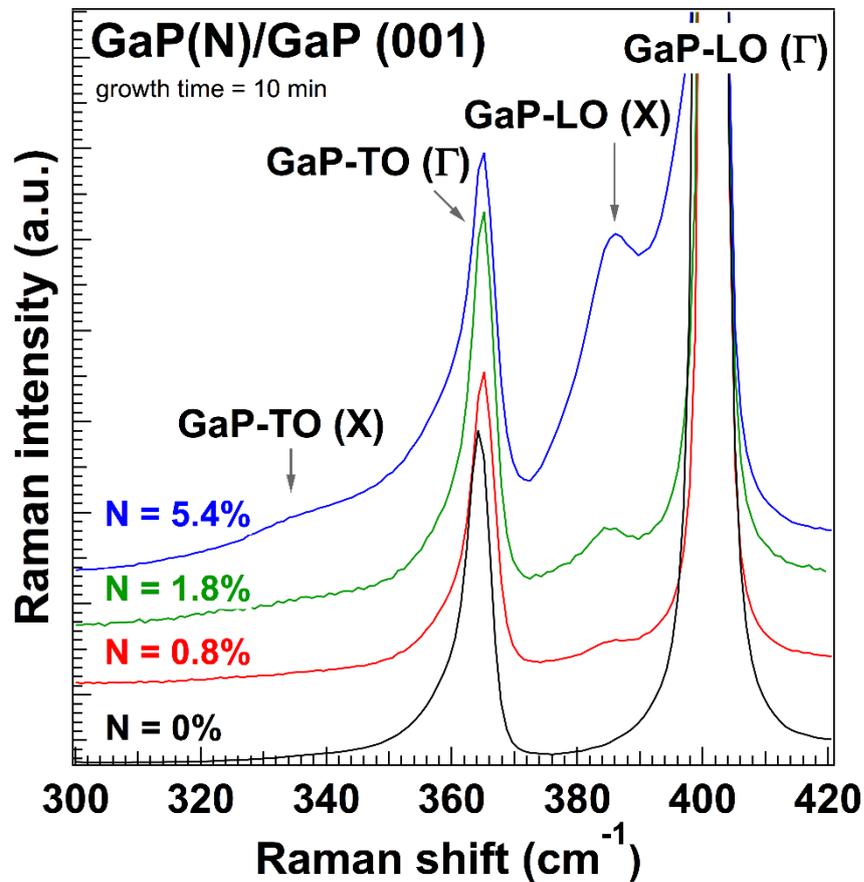
Fig. 4-8 Raman spectra of GaPN thin films grown on GaP substrate for 10 min with different N contents.

Figure 4-8 shows micro-Raman spectra in a range of 300 to 420 cm^{-1} for all the GaPN thin films grown on GaP (001) substrates for 10 min. It is clearly seen that the Raman peak located at 391 cm^{-1} significantly depends on the N content. Also, another feature are seen 336 cm^{-1}. According to the literatures, these additional features are attributed to GaP-LO (X) [28, 31] and GaP-TO (X) [32], respectively. The Raman intensities of these phonon modes are increased with N incorporation. This indicates that the two additional phonon modes are possibly used as an indicator for the N incorporation.
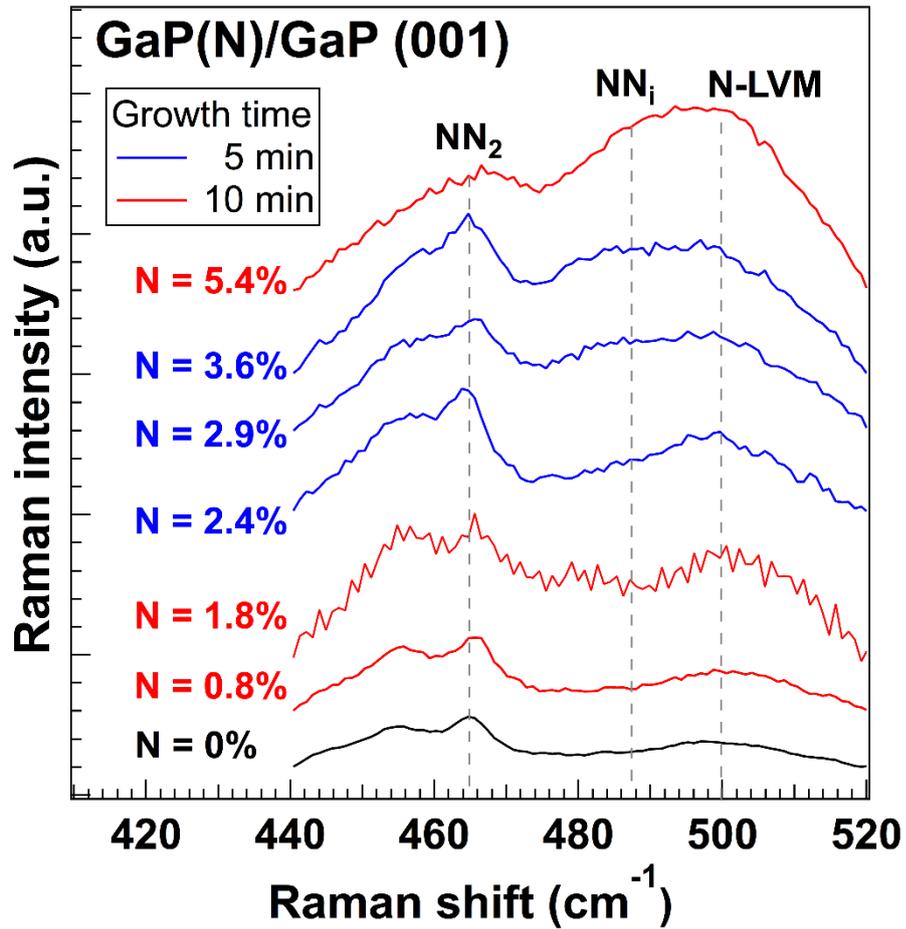
Fig. 4-9 Raman spectra of GaPN thin films on GaP substrate with the growth time of 5 min and 10 min comparing with GaP film which were represented as blue, red and black solid lines, respectively.

It is well known that if an N atom occupies P lattice site and surrounded by 4 Ga atoms, the N atoms can vibrate with the unique vibrational frequency, namely N-related localized vibrational modes (N-LVM). For GaPN system, N-LVM emerges at about 498 cm^{-1}. In addition, N-related vibrational modes (N-VMs) due to N pairs are also close the N-LVM. Figure 4-9 illustrates the Raman spectra of N-VMs of GaPN with the growth time of 5 and 10 min. In the film with low N content (N $\leq$ 0.8 at%), the spectrum is quite similar to GaP. However, the Raman intensities of N-LVM and the N pairs at various frequencies are increasing with N $\geq$ 1.8 at%.
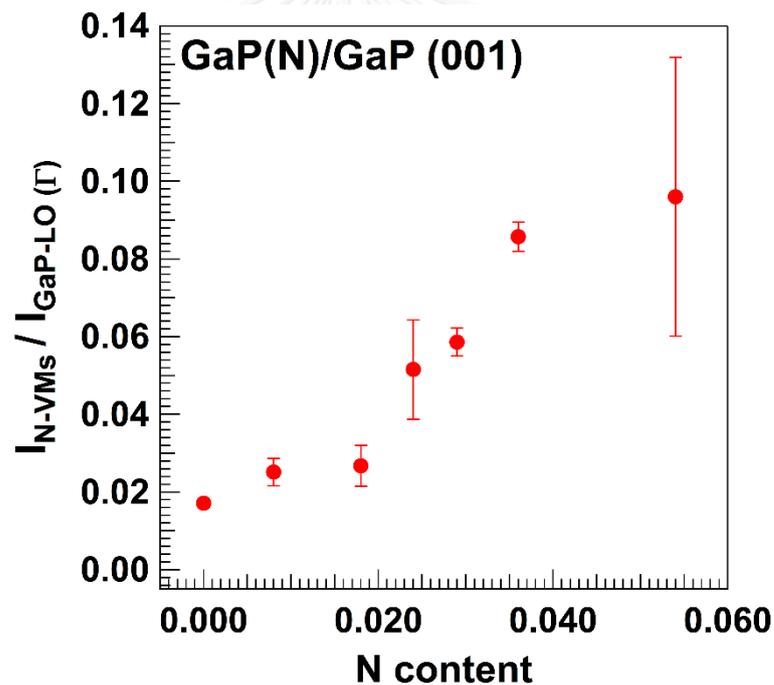
Fig. 4-10 A relationship between Raman intensities ratio of N-VMs and GaP-LO (Γ) with respect to x_{XRD} of GaPN. The error bars represent the standard deviation which indicate the distribution of five measurements.

Figure 4-10 shows the relationship between Raman intensities ratio of N-VMs and GaP-LO (Γ) with respect to x_{XRD} of GaPN. It is clearly observed that the Raman intensities ratio exhibits linear correlation with N content, indicates that the vibrational modes located in this region are relate to x_{XRD}. The graph also shows error bars that present the Raman intensities ratio distributions calculated from the Raman intensities ratio of five random location on the samples. There is explicitly observed that the error bar of GaPN with N content of 5.4 at% is very large comparing with others. This result reveals that the incorporation of N atoms is less uniformity. As described previously, the vibrational modes in range of 440 – 520 cm^{-1} also contain the Ga-P related vibrational modes. In order to confirm that the vibrational modes are directly depend on N atom, the relationship between Raman intensities and N content was determined using direct subtraction of the GaP spectrum, as shown in figure 4-11. It is found that the subtracted spectra also exhibit linear correlation with the N content, indicate that N-VMs is directly proportional to N content.

It is known that the integrated Raman intensity of GaP-LO (Γ) ($I_{GaP-LO(\Gamma)}$) in GaPN alloy is proportional to the P concentration and of N-VMs (I_{N-VMs}) are also proportional to the N concentration. The N content measured from Raman spectroscopy (x_{Raman}) can be applied from the previous publication, as follows [27]:

$$x_{Raman} = \frac{I_{N-VMs}}{f \cdot I_{GaP-LO(\Gamma)} + I_{N-VMs}},$$ (4-1)
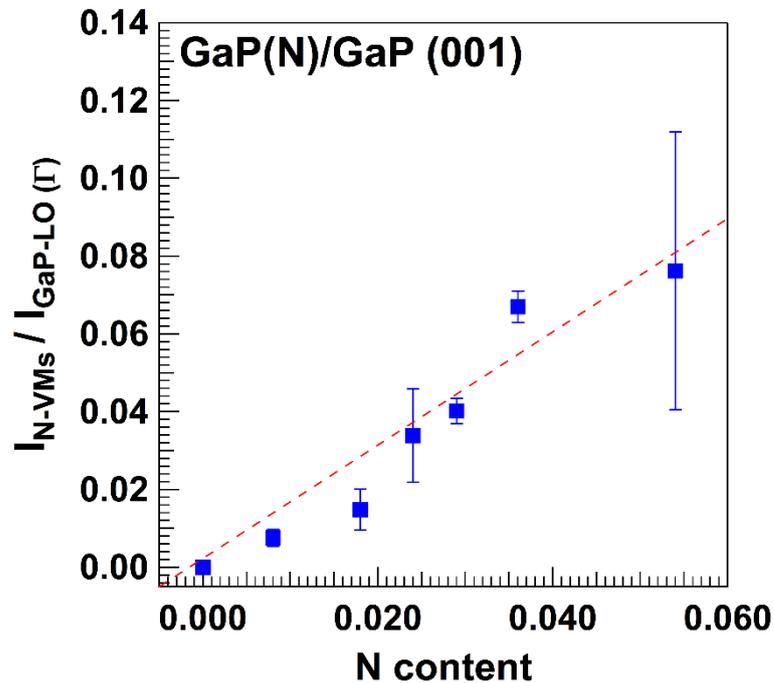
Fig. 4-11 A relationship between Raman intensities ratio of N-VMs subtracted by GaP spectrum with respect to GaP-LO (Γ) and x_{XRD} of GaPN. The error bars represent the standard deviation which indicate the distribution of five measurements.

where f symbolizes the relative scattering yield of N atoms with respect to the P atoms. $I_{GaP-LO(\Gamma)}$ and I_{N-VMs} were calculated using trapezoidal numerical integration after baselines and GaP-related vibrational modes subtraction corrections. Figure 4-12 shows the correlation between x_{Raman} and x_{XRD} using eq. 4-1 with $f = 1.0$, when error bars indicate standard deviation of five position measurements. It can be observed that the correlation also exhibits linear behavior. On the other hands, using $f = 1.6$, x_{Raman} and x_{XRD} are equally presented for N content up to $x_{XRD} = 5.4$ at%, as illustrated in figure 4-13.
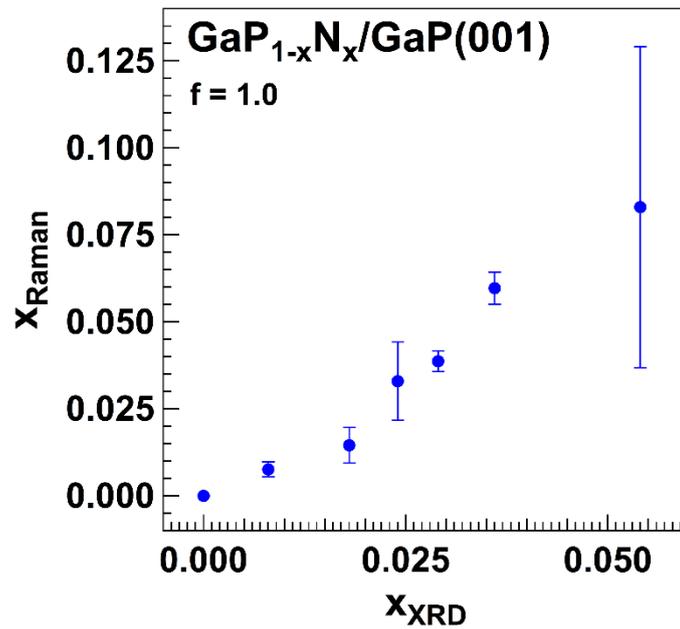
Fig. 4-12 The correlation between x_{Raman} and x_{XRD} of GaPN with x_{XRD} up to 5.4 at%.
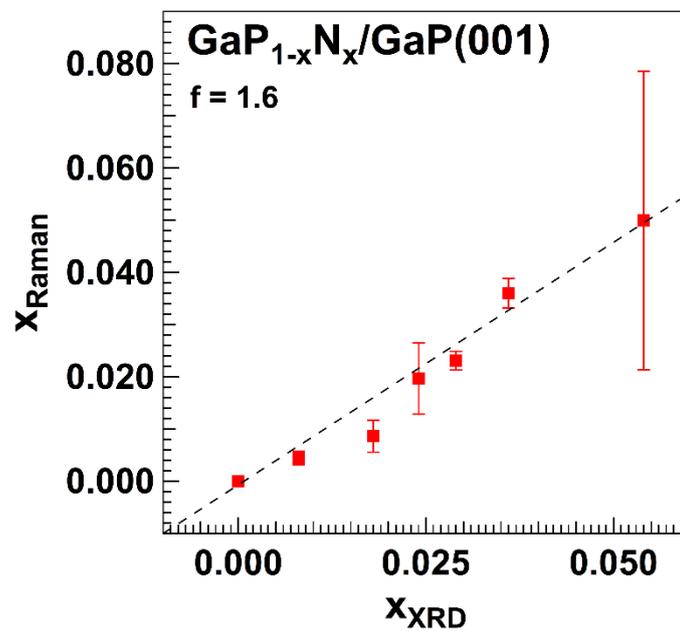
Fig. 4-13 The x_{Raman} as a function of x_{XRD} using $f = 1.6$. The dash line was shown for

guide to the eyes.

Since the assumptions of the N content finding using HRXRD and Raman spectroscopy techniques are quite difference. The 1:1 correlation between the N content obtained using HRXRD and Raman spectroscopy techniques is required to confirm that the N atoms added in the GaP host crystals are incorporated into the P lattice sites. In other words, this correlation implies that the GaPN thin films are the high quality films because few point defects as interstitial were detected.

As mentioned previously about the large N content distribution obtained by Raman scattering, Consider the results located below the average data, it is observed that N content obtained by HRXRD is higher than by Raman spectroscopy. This result indicating that some N atoms at the measured locations were located in the GaP crystals as interstitials. Whereas, the results located above the average data implied that some N atoms at the measured locations were located as the N clusters.

4.3 Optical Investigations

Consider a pure binary alloy, photoluminescence of the alloy must be generated from interband transition. Therefore, a shape spectrum should be obtained from Photoluminescence measurement. Whereas the impurity atoms containing alloy, especially GaPN, Its luminescence are consisting of carrier transition mechanisms, such as free and bound exciton to valence band transitions, conduction band to free or bound exciton state transitions, free to bound exciton transition, etc. When photoluminescence at low temperature of the samples were carried out, its spectrum was made up of these transition mechanisms. On the other hand, these mechanisms are rarely observed at room temperature. It is well known that photon energy which has the highest PL intensity refers the near band edge emission due to

higher N incorporation density with respect to other location in the film. Figure 4-14 represents the band diagram in the real space. For the simplest case, this diagram implies that the N atoms were incorporated in the crystals randomly, resulting in periodic bandgap fluctuation.
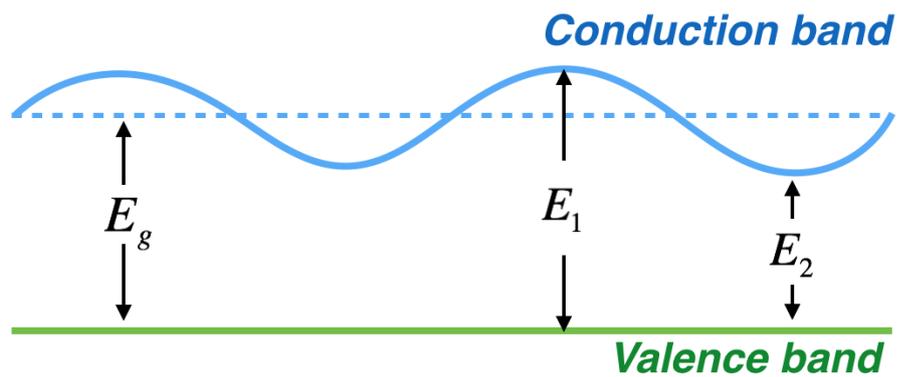
Fig. 4-14 Diagram of the periodic band edge fluctuation induced by a non-uniformity of the N incorporation.

Figure 4-15 displays the PL spectrum of GaPN for 5 min and the N content of 1.8 at%. It is clearly seen the asymmetric spectrum formed by the rough band edge as described previously. The average bandgap (E_g) can be defined as the average value of photon energy between E_1 and E_2. When, E_1 is an interception point of the tangent line and the energy axis, and E_2 is minimum photon energy that still located on the tangent line. Consider figure 4-16, after defining of the tangent line, the value of E_2 is found at 1.80 eV. The value of E_1 is defined from the midpoint between E_{1-max} and E_{1-min}. When the values of E_{1-max} and E_{1-min} are obtained from the tangent lines which are constructed at upper and lower boundaries of the noise spectrum.
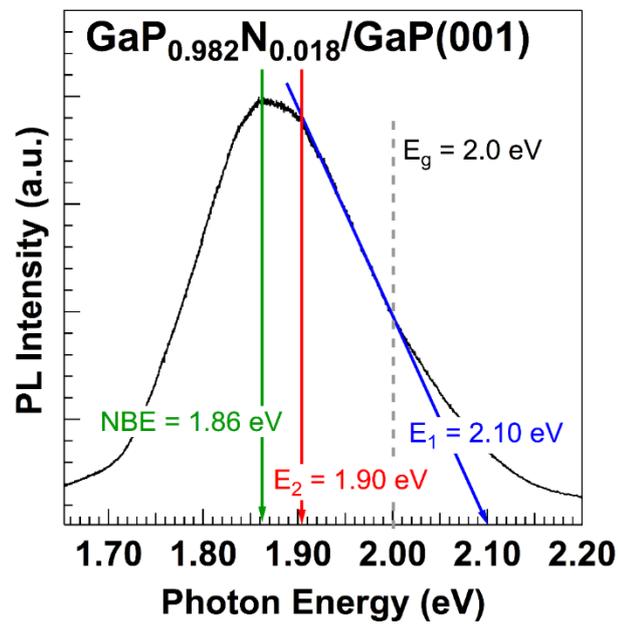
Fig. 4-15 Illustration of E_1 finding of GaPN thin film with the N content of 5.4 at%.
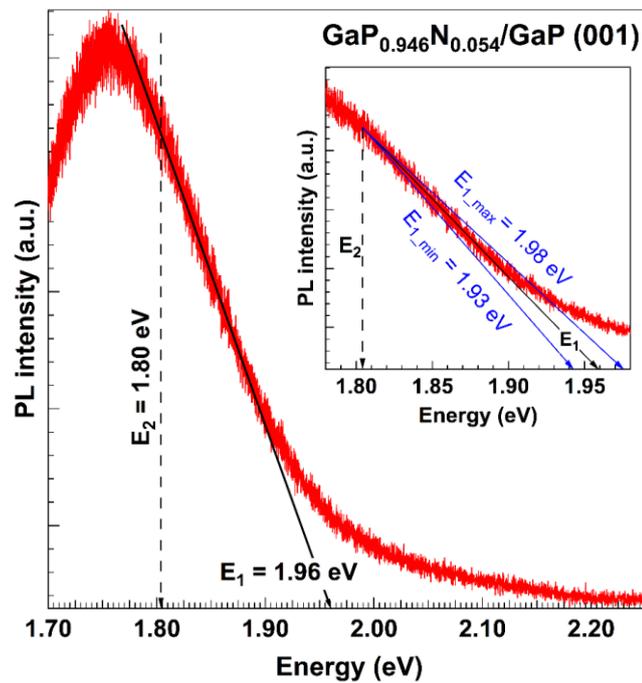
Fig. 4-16 Illustration of band gap energy finding of GaPN thin films, photon energy which has highest PL intensity refers as near band edge emission of the sample.

For example shown in figure 4-15, the tangent line is constructed at the higher energy region of the PL spectrum. E_1 and E_2 were obtained to be 2.10 and 1.90 eV, respectively. Thus the average bandgap is calculated to be 2.0 eV for GaPN with the N content of 1.8 at%.
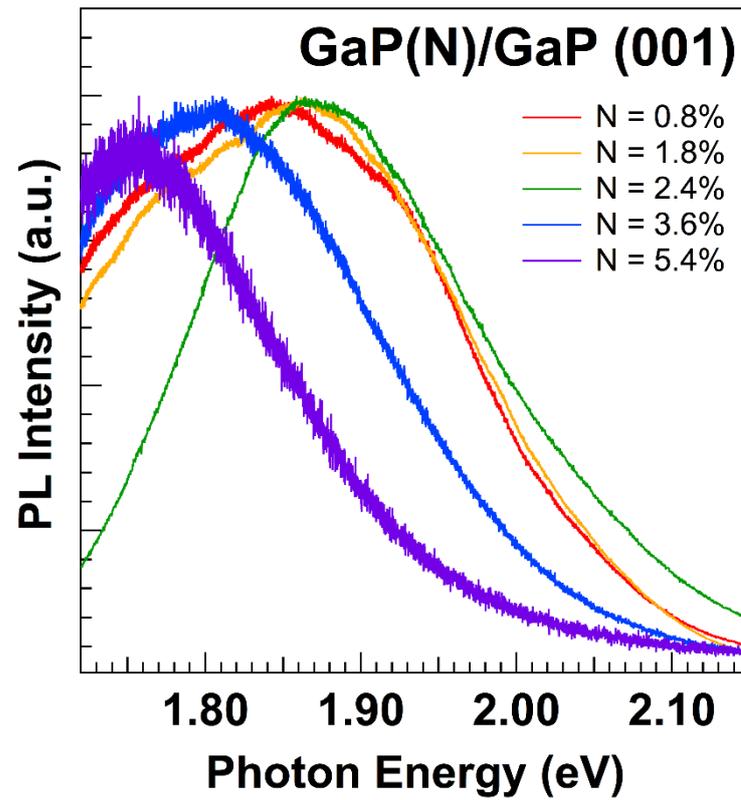
Fig. 4-17 The luminescence of GaPN films with different N contents.

Room temperature micro-photoluminescence spectroscopy was operated to investigate bandgap of GaPN thin films with the growth time of 5 and 10 min. Figure 4-17 displays the luminescence of GaPN films with different N contents. It is observed that the bandgap of the films shift to the lower energy due to an incorporation of N replaced to the P atoms. Figure 4-18 shows bandgap as a function of the N content of GaPN with the N content up to 5.4% comparing with other researchers [1, 2, 4, 11]. The bandgap of GaPN thin films measured at high temperature are slightly decrease with respect to bandgap of samples measured at low temperature. However, it is clearly observed that the bandgap of the film with the N content of 0.8 and 1.8 at% are dramatically reduced due to film relaxation effect. The film relaxation can be occurs due to the actual film thickness is higher than the critical thickness.

In additions, the uncertainty of the bandgap (ΔE_g) is calculated as follows:

$$\Delta E_g = \sqrt{(\frac{\partial E_g}{\partial E_1})^2 \cdot \Delta E_1^2 + (\frac{\partial E_g}{\partial E_2})^2 \cdot \Delta E_2^2} \qquad (4\text{-}1)$$

Certainly, ΔE_2 becomes zero and ΔE_1 is calculated from the different between the values of E_1 and $E_{1-\min}$ (or $E_{1-\max}$). Therefore, ΔE_g is obtained to be $\frac{\Delta E_1}{2}$. According to a signal to noise ratio observed on the spectrum in figure 4-16 and 4-17, ΔE_g of the film with highest the N content was calculated to be 0.03 eV.

Finally, the bowing parameter of GaPN was determined to be 10 eV using the modified Vegard's law, eq. (2-2).
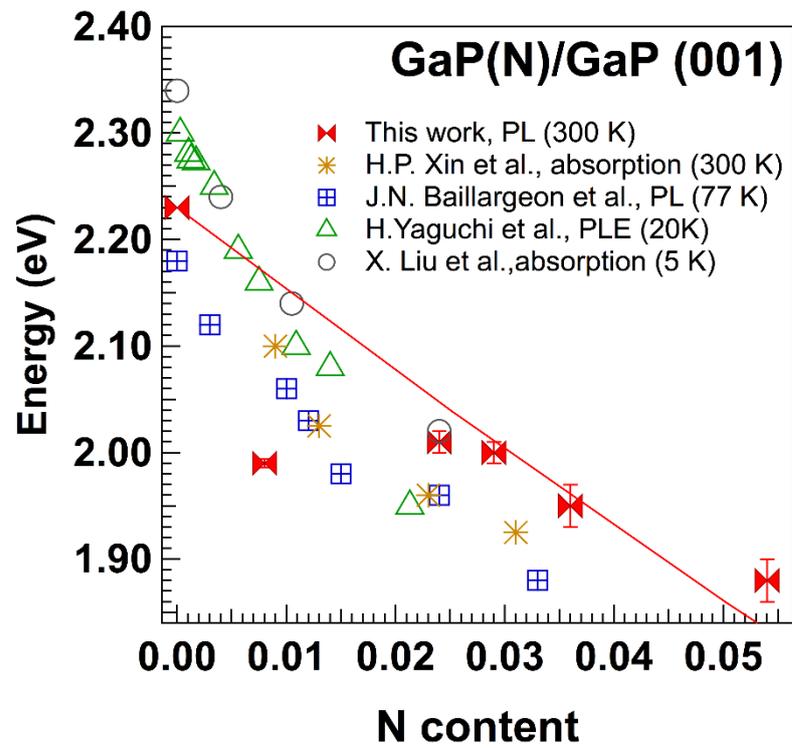
Fig. 4-18 Bandgap as a function of N content obtained by various researchers. The error bars represent the band gap energy fluctuation due to five repeating measurements.

CHAPTER V

CONCLUSIONS

In the thesis, GaPN thin films on GaP (001) substrates with N content measured by HRXRD up to 5.4 at% have been studied. The goal of the thesis is to investigate the structural and optical properties due to the N addition into GaP crystals using high resolution X-rays diffraction (HRXRD), scanning electron microscopy (SEM), atomic force microscopy (AFM), Raman spectroscopy and photoluminescence spectroscopy techniques.

The N content of GaPN thin films have been determined using HRXRD. It is found that the highest N content is 5.4 at% for the GaPN film with the highest DMHy flow rate of 300 μmol/min. The macroscopic quality of GaPN films have been investigated by SEM and AFM. It is observed that surface and interface of the thin films are fairly smooth. These results confirm that the film quality is good enough for further analysis that are the vibrational and optical investigations.

The GaPN films have been analyzed by Raman spectroscopy technique. It is found that the N-related vibrational modes are observed at around $440 - 520$ cm^{-1}. The Raman intensity ratio between N-related modes and GaP-LO (Γ) is proportional to the N content. The N content determine by Raman spectroscopy reveals a directly linear correlation on the N content measured by HRXRD using $f = 1.6$. This discovery provides that the Raman scattering is a suitable technique to determine the N content in dilute GaPN thin films.

Photoluminescence spectroscopy have been carried out to investigate the bandgap of the thin films. A dramatically reduction of the bandgap due to an incorporation of N into P lattice sites indicates a huge band gap bowing parameter of 10 eV at room temperature.

Hopefully, this study is useful to make understanding the structural and optical properties of GaPN alloy. For the further work, it is necessary to clarify the N addition on the N-related energy states at low temperature.

REFERENCES

[1]   Baillargeon, J.N., Pearah, P.J., Cheng, K.Y., Hofler, G.E. and Hsieh, K.C. *Growth and luminescence properties of GaP:N and GaP$_{1-x}$N$_x$.* Journal of Vacuum Science & Technology B. 10 (1992) : 829-831.

[2]   Liu, X., Bishop, S.G., Baillargeon, J.N. and Cheng, K.Y. *Band gap bowing in GaP$_{1-x}$N$_x$ alloys.* Applied Physics Letters, 62 (1993) : 208-210.

[3]   Bi, W.G. and Tu, C.W. *N incorporation in GaP and band gap bowing of GaN$_x$P$_{1-x}$.* Applied Physics Letters, 69 (1996) : 3710-3712.

[4]   Xin, H.P., Tu, C.W., Zhang, Y. and Mascarenhas, A. *Effects of nitrogen on the band structure of GaN$_x$P$_{1-x}$ alloys.* Applied Physics Letters, 76 (1999) : 1267-1269.

[5]   Sanorpim, S., and others *MOVPE growth and optical investigations of InGaPN alloys.* Journal of Crystal Growth, 275 (2005).

[6]   Kim, K.M., and others *Optical properties of InGaPN epilayer with low nitrogen content grown by molecular beam epitaxy.* Journal of Applied Physics, 112 (2012).

[7]   Momose, K., and others *Dislocation-free and lattice-matched Si/GaP$_{1-x}$N$_x$/Si structure for photo-electronic integrated systems.* Applied Physics Letters, 79 (2001) : 4151-4153.

[8]   Yonezu, H. *Control of structural defects in group III–V–N alloys grown on Si.* Semiconductor Science and Technology, 17 (2002) : 762-768.

[9]   Nakajima, F., Ono, W., Kuboya, S., Katayama, R. and Onabe, K. *MOVPE growth and optical characterization of GaPN films using tertiarybutylphosphine (TBP) and 1,1-dimethylhydrazine (DMHy).* Journal of Crystal Growth, 298 (2007) : 103-106.

[10]   Buyanova, I.A., Rudka, G.Y., Chen, W.M., Xin, H.P. and Tu, C.W. *Radiative recombination mechanism in GaN$_x$P$_{1-x}$ alloys.* Applied Physics Letters, 80 (2002) : 1740-1742.

[11]   Yaguchi, H., and others *Photoluminescence excitation spectroscopy of GaP$_{1-x}$N$_x$ alloys: conduction-band-edge formation by nitrogen incorporation.* Journal of Crystal Growth, 170 (1997) : 353-356.

[12]   Thomas, D.G. and Hoffield, J.J. *Isoelectronic Traps Due to Nitrogen in Gallium Phosphide.* Physical Review, 150 (1966) : 680-689.

[13]   Odnoblyudov, V. A. and Tu, C.W. *Amber GaNP-based light-emitting diodes directly grown on GaP(100) substrates.* Journal of Vacuum Science & Technology B, 24 (2006) : 2202-2204.

[14]   Hatakenaka, S., Nakanishi, Y., Wakahara, A., Furukawa, Y. and Okada, H. *Doping control and evaluation of pn-junction LED in GaPN grown by OMVPE.* Journal of Crystal Growth, 310 (2008) : 5147-5150.

[15]   Xin, H.P., Welty, R.J. and Tu, C.W. *GaN$_{0.011}$P$_{0.989}$ red light-emitting diodes directly grown on GaP substrates.* Applied Physics Letters, 77 (2000) : 1946-1948.

[16]   Moon, S.Y., and others *GaPN–GaP double heterostructure light emitting diode grown on GaP substrate by solid-source molecular beam epitaxy.* Physica Status Solidi (a), 201 (2004) : 2695-2698.

[17] Peternai, L., Kováč, J., Jakabovič, J., Gottschalch, J.V. and Rheinlaender, B. *Investigation of GaN$_x$P$_{1-x}$/GaP LED Structure Optical Properties.* Journal of Electronic Materials, 35 (2006) : 654-657.

[18] Peternai, L., and others *Optical and Structural investigation of GaN$_x$P$_{1-x}$/GaP structures for light emitting diodes.* Vacuum, 80 (2005) : 229-235.

[19] Bachrach, R.Z., Joyce, W.B. and Dixon, R.W. *Optical-coupling efficiency of GaP:N green-light-emitting diodes.* Journal of Applied Physics, 44 (1973) : 5458-5462.

[20] Zdánský, K., Zavadil, J., Nohavica, D. and Kugler, S. *Degradation of commercial high-brightness GaP:N green light emitting diodes.* Journal of Applied Physics, 83 (1998) : 7678-7684.

[21] Chamings, J., Ahmed, S., Sweeney, S.J., Odnoblyudov, V.A. and Tu, C.W. *Physical properties and efficiency of GaNP light emitting diodes.* Applied Physics Letters, 92 (2008).

[22] Stringfellow, G.B. *Calculation of Ternary and Quaternary III-V Phase Diagrams.* Journal of Crystal Growth, 27 (1974) : 21-34.

[23] Vurgaftman, I., Meyer, J.R. and Ram-Mohan, L.R. *Band parameters for III-V compound semiconductors and their alloys.* Journal of Applied Physics, 89 (2000) : 5815-5875.

[24] Yaguchi, H. *Theoretical study of conduction band edge formation in GaP$_{1-x}$N$_x$ alloys using a tight-binding approximation.* Journal of Crystal Growth, 189/190 (1998) : 500-504.

[25] McCluskey, M.D. *Local vibrational modes of impurities in semiconductors.* Journal of Applied Physics, 87 (2000) : 3593-3617.

[26] Seong, M.J., Hanna, M.C. and Mascarenhas, A. *Composition dependence of Raman intensity of the nitrogen localized vibrational mode in GaAs$_{1-x}$N$_x$.* Applied Physics Letters, 79 (2001) : 3974-3976.

[27] P. Panpech, and others *Correlation between Raman intensity of the N-related local vibrational mode and N content in GaAsN strained layers grown by MOVPE.* Journal of Crystal Growth, 298 (2007) : 107-110.

[28] Vorlíček, V., Gregora, I., Riede, V. and Neumann, H. *Raman Scattering study of GaP:N Epitaxial Layers.* Journal of Physics and Chemistry of Solids, 49 (1988) : 797-805.

[29] Sushchinsky, M.M., Gorelik, V.S. and Maximov, O.P. *Higher-order Raman Spectra of GaP.* Journal of Raman Spectroscopy, 7 (1978) : 26-30.

[30] Hoff, R.M. and Irwin, J.C. *Second-Order Raman Spectra and Phonon Dispersion in GaP.* Canadian Journal of Physics, 51 (1972) : 63-76.

[31] Buyanova, I.A., Chen, W.M., Goldys, E.M., Xin, H.P. and Tu, C.W. *Structural properties of a GaN$_x$P$_{1-x}$ alloy: Raman studies.* Applied Physics Letters, 78 (2001) : 3959-3961.

[32] Nagarajan, S., and others *Strain-compensated GaPN/GaP heterostructure on (001) silicon substrates for intermediate band solar cells.* Journal of Physics D: Appiled Physics, 46 (2013).

VITA

Mr. Noppadon Toongyai was born on April 30, 1990 in Lop buri, Thailand. He received his Bachelor degree of Science in Physics from Chulalongkorn University in 2011, and continued his Master's study in 2012.

Conference Presentations:

1. N. Toongyai, S. Sanorpim and K. Onabe, 'Raman scattering from nitrogen-related vibrational modes in high nitrogen content GaPN grown by MOVPE', 39th congress on science and technology of Thailand, Thailand, October 21-23, 2013. (oral presentation)

2. N. Toongyai, S. Sanorpim and K. Onabe, 'Raman scattering from nitrogen-related vibrational modes in high nitrogen content GaPN grown by MOVPE', 9th Mathematics and physical science graduate conference, Malaysia, January 8-10, 2014. (oral presentation)

3. N. Toongyai, S. Sanorpim, K. Onabe, 'N-induced vibrational modes and optical property of high nitrogen-content GaPN grown by MOVPE', 9th Annual conference of the thai physics society, Thailand, March 26-29, 2014. (oral presentation)

4. N. Toongyai, S. Sanorpim, K. Onabe, 'Raman scattering of the N-related vibrational modes in high N-content GaPN films grown on GaP (001) substrates by MOVPE', 10th Annual conference of the thai physics society, Thailand, May 20-22, 2015. (poster presentation)